

BOSTON UNIVERSITY  
SCHOOL OF MEDICINE

Thesis

**ANALYTICAL FIGURES OF MERIT AS A MEANS TO COMPARE METHODS:  
AN EXAMPLE USING LATERAL FLOW IMMUNOCHROMATOGRAPHIC  
TEST STRIPS AND REAL-TIME PCR**

by

**CRYSTAL MAE (SIMSON) OECHSLE**

B.S., Ohio University, 2007

Submitted in partial fulfillment of the  
requirements for the degree of  
Master of Science

2011

Approved By

First Reader

---

Catherine M. Grgicak, Ph.D.  
Instructor Biomedical Forensic Sciences

Second Reader

---

Amy L. Barber, M.S.  
DNA Unit Supervisor & Acting Technical Leader  
Massachusetts State Police Crime Laboratory

## **Acknowledgements**

I would like to express my sincere gratitude to all those individuals who provided me with their reassurance, guidance, and expertise throughout the course of this project. Without their support, this thesis would not have come to fruition. I would specifically like to thank my husband, Stephan, for his endless encouragement; my co-workers at the Massachusetts State Police, including Amy Barber, Sandra Haddad, Joanne Sgueglia, Kristen Sullivan, and Maureen McCabe, for their commitment to excellence in the field of forensics; and my advisor at Boston University, Catherine Grgicak, for her time, patience, and direction.

**ANALYTICAL FIGURES OF MERIT AS A MEANS TO COMPARE METHODS:  
AN EXAMPLE USING LATERAL FLOW IMMUNOCHROMATOGRAPHIC  
TEST STRIPS AND REAL-TIME PCR  
CRYSTAL MAE (SIMSON) OECHSLE**

Boston University School of Medicine, 2011

Major Professor: Catherine M. Grgicak, Ph. D., Instructor  
Biomedical Forensic Sciences

**ABSTRACT**

Forensic evidence samples are often subjected to a variety of biological fluid identification methods before potentially probative items are forwarded to DNA analysis. Serologically based screening techniques may provide valuable insight in how to proceed with a specific sample; however, they consume a vital portion of the available evidence. One limitation of these techniques is that they are qualitative or semi-quantitative in nature, relying on visual interpretation by analysts. In contrast, recent advances in real-time Polymerase Chain Reaction (PCR) quantification allow for the simultaneous detection of total human and male DNA. Commercially available quantification kits do not identify bodily fluids, per se, but do yield information regarding the proportion of the DNA present in the sample and the downstream amplifiability of the genetic material. Therefore, real-time quantification could theoretically be used as a screening method for subsequent PCR amplification of human specific Short Tandem Repeat (STR) DNA profiles. This type of analytical scheme would be valuable in cases where

development of a male DNA profile, especially in the abundance of female genetic material, is probative.

In this study, dilution series of either semen or male saliva were prepared in either buffer or female blood. Semen and saliva dilution samples were subjected to lateral flow immunochromatographic test strips for the detection of either semenogelin or salivary  $\alpha$ -amylase, respectively. All samples were also subjected to real-time PCR analysis, which allowed for simultaneous quantification of total human and male DNA. Because the chemistries and signal outputs of each method differs, a direct comparison of signal could not be made. Instead, analytical figures of merit based on the volume of bodily fluid were evaluated. With the exception of the semen dilution series analyzed on the immunoassay cards, which displayed evidence of the high-dose hook effect, log-linear relationships between signal and volume were observed for both platforms. Utilizing this relationship and the theory of the propagation of random errors the Limits of Detection (LOD) were determined to be 0.05  $\mu$ L of saliva for the RSID™ Saliva cards, 0.03  $\mu$ L saliva for Quantifiler® Duo, and 0.001  $\mu$ L of semen for Quantifiler® Duo. Due to its stability in various matrices, sensitivity, low limits of detection, and reproducibility, quantitative PCR is a viable and effective screening method for subsequent DNA profiling.

## Table of Contents

Title Page	i
Reader's Approval Page	ii
Acknowledgements	iii
Abstract	iv
Table of Contents	vi
List of Tables	viii
List of Figures	x
List of Abbreviations	xii
Introduction	1
<i>Immunochromatographic Test Strips</i>	3
<i>Real-Time PCR</i>	7
Materials & Methods	13
<i>Body Fluid Dilution Series</i>	13
<i>Extraction for Amylase</i>	15
<i>Extraction for Sperm Cells and Semenogelin</i>	16
<i>Immunochromatographic Test Strips &amp; ImageJ</i>	17
<i>Organic Extraction of DNA</i>	19
<i>Real-Time PCR</i>	20
Results & Discussion	22
<i>Raw Data</i>	22
<i>Matrix Effects &amp; Sensitivity</i>	33

<i>Overall Limits of Detection</i>	40
<i>Reproducibility</i>	50
Conclusions & Future Work	53
Bibliography	56
Curriculum Vitae	64

## List of Tables

<b>Table 1.</b> List and preparation of the 11 samples in each body fluid dilution series. Values in parenthesis represent dilutions of the body fluid of interest prior to its addition to the mixture.	14
<b>Table 2.</b> Immunoassay card MBS and standard deviation values used to calculate MDS values (shown in bold), which are plotted as dashed horizontal lines in Figures 9A (saliva-blood and saliva-TE) and 9B (semen-blood and semen-TE) and later in Figures 11A (saliva) and 11B (semen).	30
<b>Table 3.</b> Calibration sensitivities for body fluid dilution series analyzed with RSID™ Saliva cards, RSID™ Semen cards, and Quantifiler® Duo.	34
<b>Table 4.</b> Analytical sensitivities for Saliva-Blood dilution series analyzed with RSID™ Saliva cards and Quantifiler® Duo.	35
<b>Table 5.</b> Analytical sensitivities for Saliva-TE dilution series analyzed with RSID™ Saliva cards and Quantifiler® Duo.	35
<b>Table 6.</b> Analytical sensitivities for Semen-Blood dilution series analyzed with RSID™ Semen cards and Quantifiler® Duo.	36
<b>Table 7.</b> Analytical sensitivities for Semen-TE dilution series analyzed with RSID™ Semen cards and Quantifiler® Duo.	36
<b>Table 8.</b> Overall calibration sensitivities for RSID™ Saliva cards, RSID™ Semen cards, and Quantifiler® Duo.	39
<b>Table 9.</b> Presence of signal – either a red band in the test region for immunoassay cards or a C <sub>T</sub> value for real-time PCR – in detection of Saliva.	41
<b>Table 10.</b> Presence of signal – a red band in the test region for immunoassay cards, sperm on microscope slides, or a C <sub>T</sub> value for real-time PCR – in detection of Semen.	42
<b>Table 11.</b> Limits of Detection of saliva and semen for the various detection methods.	46



**Table 12.**  $F_{\text{test}}$  values comparing sample variance seen on RSID™ immunoassay cards with the corresponding Quantifiler® Duo sample variance.

51

## List of Figures

<b>Figure 1.</b> Illustration of the principle behind the production of a red-band in the test region of immunoassay cards using colloidal gold labeled antibodies.	6
<b>Figure 2.</b> Illustration of lateral flow immunochromatographic test strip mechanism.	6
<b>Figure 3.</b> Illustration of the three phases of real-time PCR: exponential, linear, and plateau. The Cycle Threshold ( $C_T$ ), or the cycle number at which fluorescence crosses a set threshold, is also depicted.	8
<b>Figure 4.</b> Illustration of the Taqman <sup>®</sup> probe detection method of real-time PCR.	11
<b>Figure 5.</b> Flow chart of sample preparation for body fluid mixtures.	15
<b>Figure 6.</b> (A) Third replicate of the saliva-TE dilution series run on RSID <sup>™</sup> Saliva lateral flow immunochromatographic test strips. (B) Third replicate of the semen-blood dilution series run on RSID <sup>™</sup> Semen lateral flow immunochromatographic test strips.	23
<b>Figure 7.</b> ImageJ software output for the third replicate of the semen-blood 1:50 dilution (immunoassay card seen in Figure 6).	24
<b>Figure 8.</b> Real-time PCR amplification plots for the third replicate of the semen-blood dilution series. The horizontal green line represents the signal intensity threshold needed for the $C_T$ to be recorded.	27
<b>Figure 9.</b> Sensitivity curves for immunochromatographic test strips and real-time PCR quantification platforms. (A) Saliva-Blood and Saliva-TE dilution series on RSID <sup>™</sup> Saliva cards, (B) Semen-Blood and Semen-TE dilution series on RSID <sup>™</sup> Semen cards, (C) Saliva-Blood and Saliva-TE dilution series with Quantifiler <sup>®</sup> Duo, and (D) Semen-Blood and Semen-TE dilution series with Quantifiler <sup>®</sup> Duo.	29

<b>Figure 10.</b> Determination of error for the 40 C <sub>T</sub> MBS by modeling the errors of the 8 points (A – H) in the real-time PCR standard curve.	32
<b>Figure 11.</b> RSID™ immunoassay card calibration sensitivity plotted against Quantifiler® Duo calibration sensitivity. (A) Overall Saliva and (B) Overall Semen.	39
<b>Figure 12.</b> RSID™ immunoassay card RSDs plotted against Quantifiler® Duo RSDs. (A) Overall Saliva and (B) Overall Semen.	52

### **List of Abbreviations**

$^{\circ}\text{C}$	Degrees Celsius
$C_T$	Cycle Threshold
CCD	Charge Coupled Device
CODIS	Combined DNA Index System
DNA	Deoxyribonucleic Acid
DTT	Dithiothreitol
FBI	Federal Bureau of Investigation
fg	Femtogram
FRET	Fluorescent Resonance Energy Transfer
HPV	Human Papillomavirus
IgG	Immunoglobulin G
IUPAC	International Union of Pure and Applied Chemistry
JPEG	Joint Photographic Experts Group image
L	Liter
LOD	Limit of Detection
LSPR	Localized Surface Plasmon Resonance
MBS	Mean Blank Signal
MDS	Minimum Distinguishable Signal
$\mu\text{L}$	Microliter
mg	Milligram
mL	Milliliter

MSPCL	Massachusetts State Police Crime Laboratory
ng	Nanogram
nL	Nanoliter
NIH	National Institute of Health
OD	Optical Density
PCI	Phenol-Chloroform Isoamyl alcohol
PCR	Polymerase Chain Reaction
pg	Picogram
ProK	Proteinase K
qPCR	Quantitative Polymerase Chain Reaction
R <sup>2</sup>	Correlation Coefficient
RNA	Ribonucleic Acid
RPM	Revolutions per Minute
RPPH1	Ribonuclease P RNA Component H1
RSD	Relative Standard Deviation
RSID	Rapid Stain Identification
Sg	Semenogelin
SRY	Sex-determining Region Y
STR	Short Tandem Repeat
SWGDM	Scientific Working Group on DNA Analysis Methods
Taq	<i>Thermus aquaticus</i>
TE	Tris-EDTA (Ethylenediamine Tetra-Acetic acid)

TEG	Tris-EDTA with Glycogen
TEN	Tris-EDTA with NaCl
TES	Tris-EDTA with Sarkosyl
UV	Ultra-Violet

## **Introduction**

Forensic evidence samples are often subjected to a variety of biological fluid identification methods before potentially probative items are forwarded for DNA analysis. Serologically based screening techniques may provide valuable insight on how to proceed with a specific sample; however, they consume a significant portion of the available evidence. Another limitation of these techniques is that they are qualitative or semi-quantitative in nature, relying on visual interpretation by analysts. In contrast, recent advances in real-time PCR quantification chemistries allow for the simultaneous fluorescent detection of total human and male DNA. Where real-time PCR does not identify body fluids, per se, it can yield information on the proportion of the biological components present in the sample and the downstream amplifiability of the genetic material. Therefore, real-time quantification could theoretically be used as a screening method for subsequent PCR amplification of human-specific STR DNA profiles, and due to Standard 9.4 of the FBI's Quality Assurance Standards for Forensic DNA Testing Laboratories, real-time PCR is already validated for use by many forensic laboratories [1].

Real-time quantification with a dual human and male platform would be particularly valuable as a diagnostic approach in cases where development of a male DNA profile, especially in the abundance of female genetic material, is probative. Such a scenario often occurs with sexual assaults, which make up a significant portion of DNA backlogs. As an example, sexual assaults accounted

for approximately 7% of all violent crime nationally in 2009 [2]. Evidence related to sexual assault cases poses a unique analytical challenge because of the vast number of scenarios encountered, which is one reason why biological screening methods are commonly utilized in forensic laboratories. At the Massachusetts State Police Crime Laboratory, for instance, the current protocol for processing sexual assault evidence collection kits involves extraction and microscopic examination for the presence of sperm cells, which is typically followed by semenogelin and/or amylase testing [3-7]. This is all before an item is even submitted for DNA analysis, which consists of its own separate extraction and quantification steps. It is recognized that such an approach is redundant, timely, and not cost effective; however, there is little available in the literature that directly compares the technologies to assess whether qPCR can effectively replace traditional screening methods. Any proposed procedure that would replace serology would need to be at least as sensitive, and have a comparable limit of detection. Sensitivity and limits of detection are two important analytical criteria in sexual assault evidence examination because, as previously mentioned, these cases often involve low levels of the male biological material of interest mixed with an overwhelming amount of female biological material. A high female to male ratio can occur for a number of reasons including digital penetration, lack of ejaculation, and the reportedly high frequency of azoospermia (i.e. the absence of spermatozoa in semen) in the general population [8].



The goal of the following set of experiments is to collect data that will support or refute a method for streamlining the processing of sexual assault evidence collection kits, where traditional evaluation of sperm cells and proteins is replaced with a human and male specific dual quantification method thus saving time, energy, and resources. In this study, multiple dilution series of either semen or male saliva were prepared in either TE buffer or female blood. Semen and saliva dilution samples were subjected to RSID™ lateral flow immunochromatographic test strips for the detection of either semenogelin or salivary  $\alpha$ -amylase, respectively. Results were determined visually as well as through the use of ImageJ software, which is freeware available from the National Institute of Health (NIH) [9]. All dilution samples were also subjected to real-time PCR quantification with Quantifiler® Duo, a human and male multiplex quantification chemistry.

#### *Immunochromatographic Test Strips*

The chemistries, analytes, and signal outputs of both immunochromatographic test strips and real-time PCR differ. To appreciate these differences, an understanding of the theory behind each is needed. Immunoassay cards function on the basic principles of antibody-antigen chemistry. Antigens – sometimes called immunogens – are any substance that stimulates an immune response in the body or reacts with an antibody, and antibodies – sometimes called immunoglobulins – are Y-shaped molecules used by the immune system and produced by white blood cells to identify, neutralize,

and eliminate antigens [10]. The portion of the antigen that is recognized by the antibody is called the epitope, and if an antigen has more than one epitope, it is referred to as multivalent [11]. In contrast, most antibodies are bivalent, meaning they have two, and only two, active sites that can bind to antigens [11]. The antibody-antigen binding process is rapid, reversible, and specific. Specificity is conferred based on the amino acid sequence and structure of the active sites and epitopes involved and is sometimes referred to as a lock-and-key model, which is based on hydrogen bonding, hydrophobic interactions, and van der Waals forces [11]. The specificity of the antibody's active sites can be classified as monoclonal or polyclonal: monoclonal antibodies react with a single epitope of an antigen, but polyclonal antibodies can bind to different sites on an antigen [11]. The body's natural immune response is the release of soluble polyclonal antibodies, which can form cross-linked antibody-antigen complexes that trigger precipitation and agglutination reactions [10].

RSID™ Saliva cards detect human salivary  $\alpha$ -amylase antigen, a constituent of saliva, while RSID™ Semen Cards detect human semenogelin antigen, a constituent of semen. It is important to note that both of these lateral flow immunochromatographic test strips work in the same manner, and furthermore, both cards detect the presence of the analyte, not its activity. Using the RSID™ Semen cards as an example, the following is a discussion of the mechanism behind these immunoassay cards.

The extract-buffer mixture of interest is added to the sample well of an immunoassay cassette. The sample well of each card also contains mobile monoclonal mouse antibodies tagged with colloidal gold. Colloidal gold is a gold nanoparticle that can produce a red color due to a phenomenon known as localized surface plasmon resonance (LSPR) that occurs when many of the individual nanoparticles come into close proximity [12-14]. If semenogelin is present in a sample, it will form a complex with the gold-labeled monoclonal antibodies. The complexed antibodies, as well as extra free antibodies, are wicked up the test strip by capillary action [14]. Anti-semenogelin antibodies are immobilized in the test region of each card to capture the semenogelin antigen-antibody-colloidal gold complexes. The formation of these antibody-antigen-antibody sandwiches brings the multiple gold nanoparticles close enough together to allow them to participate in LSPR, which produces a red band in the test region [14]. Figure 1 shows a partial reproduction of a figure from Tanaka et al. [14] which illustrates how the red band is produced in the test region via colloidal gold labeled antibodies. In theory, the more analyte that is present in the sample, the darker the red band in the test region will appear. The extra free monoclonal mouse antibodies continue to move up the test strip, past the test region to the control region. Immobilized Anti-mouse IgG antibodies form a complex with the extra free monoclonal mouse antibodies and produce a red band in the control region. A red band must appear in the control region of each card to ensure that the test is working correctly [15]. See Figure 2 for an

illustration of the lateral flow immunochromatographic test strip cards and mechanism.

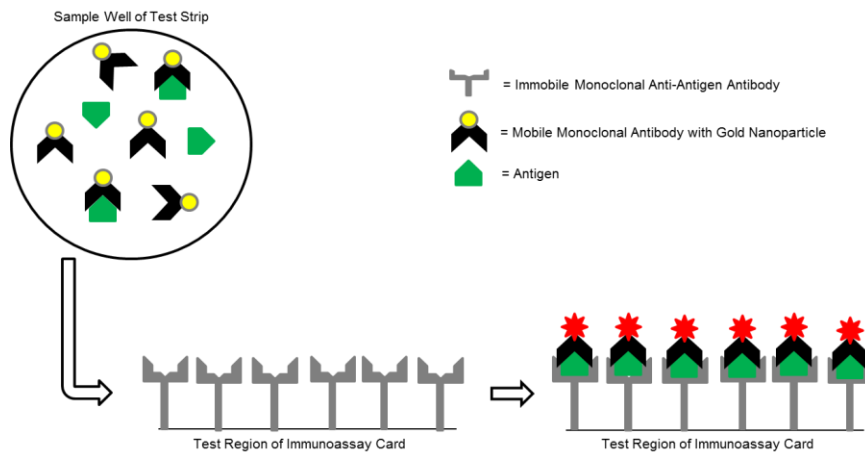


**Figure 1.** Illustration of the principle behind the production of a red-band in the test region of immunoassay cards using colloidal gold labeled antibodies.

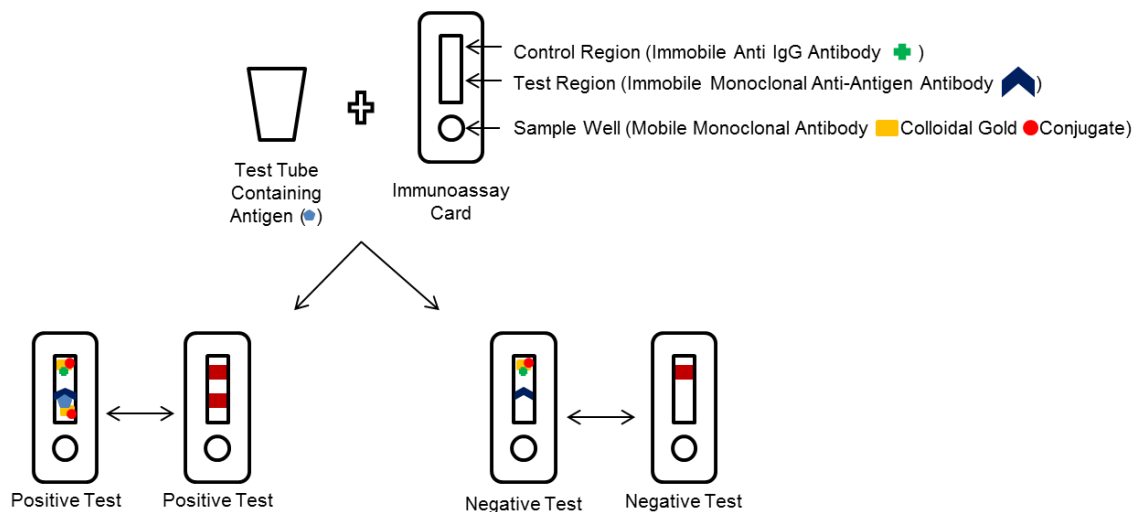


**Figure 2.** Illustration of lateral flow immunochromatographic test strip mechanism.

### *Real-Time PCR*

In contrast with the lateral flow immunochromatographic test strips, which detect the presence of specific characteristic proteins, the analyte being measured in real-time PCR is genetic material, i.e. DNA or RNA. The Polymerase Chain Reaction (PCR), first described by Mullis et al. [16], is an in vitro reaction that mimics the body's own mechanism for duplicating DNA, so that millions of copies of specific sequences of interest can be produced via a three step amplification cycle, which includes denaturation, primer annealing, and primer extension. Theoretically, at 100% efficiency, each amplification cycle should double the number of copies of the target sequence. However, the PCR is limited by the amount of primers and nucleotides present, deactivation of the polymerase, reannealing of product strands, etc. As a result, instead of the PCR exhibiting a constant exponential increase in DNA concentration, with a theoretical doubling of products, there are actually three phases: exponential, linear, and plateau. Figure 3 is a partial reproduction of a figure from *Forensic DNA Typing* by Butler, which illustrates these phases [17].

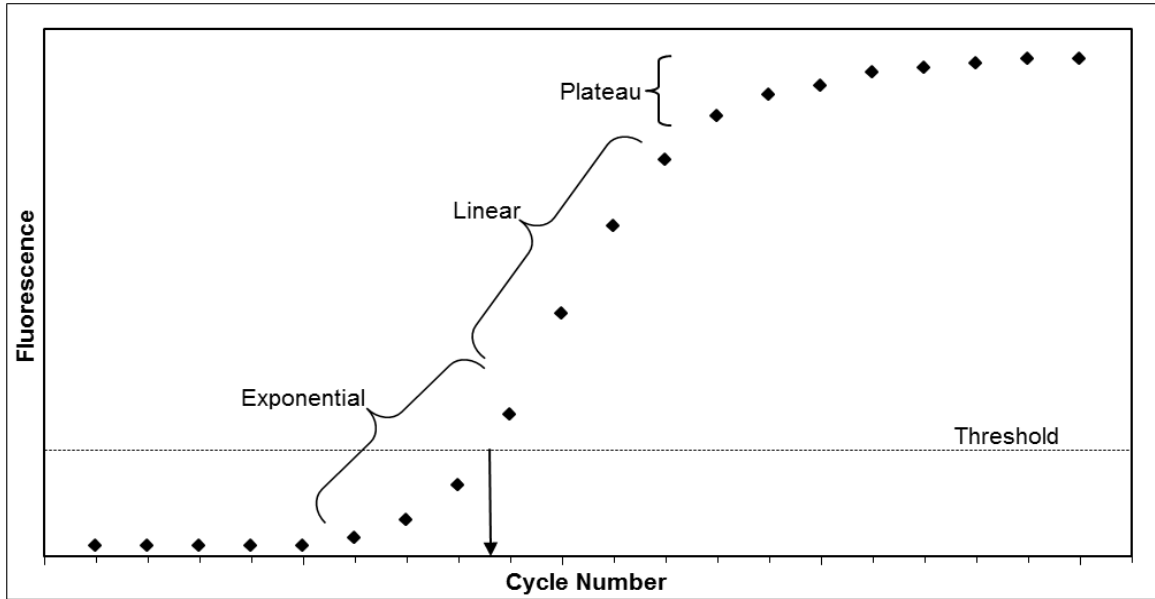


**Figure 3.** Illustration of the three phases of real-time PCR: exponential, linear, and plateau. The Cycle Threshold ( $C_T$ ), or the cycle number at which fluorescence crosses a set threshold, is also depicted.

Again, in the exponential phase, there is a high and constant efficiency, which produces a theoretical doubling of products as described by the equation:

$$C_N = C_0(1 + E)^N \quad (\text{Equation 1})$$

where  $C_N$  is the DNA concentration after a given cycle,  $C_0$  is the initial DNA concentration,  $E$  is the efficiency of the reaction, and  $N$  is the cycle number [17].

Assuming 100% efficiency, Equation 1 simplifies to Equation 2:

$$C_N = C_0 2^N \quad (\text{Equation 2})$$

In the linear phase of the PCR, copies of the target sequence are still produced, but there is no longer a doubling with each cycle as the components of the reaction become limited. In the plateau phase, the PCR reaction is significantly slowed or stopped. Therefore, if measured in the exponential phase, PCR can be incorporated into methods that quantify DNA since products produced in the

exponential phase are proportional to the initial amount of template present in the reaction.

Real-time PCR is a method that measures the increase in amplicon concentration in real-time (i.e. per cycle). This is accomplished by utilizing instrumentation which allows for fluorescence detection generated after each amplification cycle instead of at the end of the entire reaction. Endpoint detection, especially in the plateau phase, is not a suitable method for quantification due to the fact that slight differences in the reaction composition, thermal cycler conditions, and early mispriming events can cause individual reactions to exit the exponential phase at slightly different intervals [18]. In Higuchi's et al. original real-time method, ethidium bromide, an intercalating dye, was used to bind to the double stranded DNA that was produced by each PCR amplification cycle, and the fluorescence was recorded by a UV detector and a CCD [19]. Current real-time PCR detection methods, like those employed by the Quantifiler<sup>®</sup> Duo chemistry used in this study, differ from Higuchi's original design in that they exploit the 5' → 3' exonuclease activity of *Thermus aquaticus* (Taq), a DNA polymerase, and utilize a Taqman<sup>®</sup> probe with Fluorescent Resonance Energy Transfer (FRET) technology [20, 21].

The Taqman<sup>®</sup> probe is a DNA oligonucleotide, which binds to the target DNA, and has three modifications: a fluorescence emitting dye at the 5' end (a reporter), a fluorescence quenching dye at the 3' end (a quencher), and a minor groove binder at the 3' end that facilitates the binding of the probe at high

annealing temperatures. FRET refers to the use of two fluorophores with overlapping excitation and emission spectra. When the two fluorophores are in close proximity to each other, as is such when they are linked to the ends of the Taqman<sup>®</sup> probe, if the reporter is excited, there will be an energy transfer to the quencher, which will mask any fluorescence produced by the reporter. If the two fluorophores are not in close proximity (i.e. free in solution) this quenching of signal does not occur, and the light emitted from the reporter is detected. This FRET is incorporated into real-time PCR via the following mechanism. When the template DNA is denatured, primers bind to both the forward and reverse strands, but the Taqman<sup>®</sup> probe binds only to the forward strand. The Taq polymerase binds both the forward and reverse strands and synthesizes the reverse strand in the normal manner. The forward strand with the probe is also copied. However, when the polymerase encounters the Taqman<sup>®</sup> probe, the Taq Polymerase's 5' → 3' exonuclease activity ensues and degrades the probe. This action frees the reporter from the quencher. The released reporter then accumulates in solution and fluoresces, and the increase in fluorescence with each amplification cycle is recorded. The fluorescence increases proportionally with each cycle as the amount of PCR product increases, and the cycle number at which it crosses a set threshold, or the C<sub>T</sub> value, is measured (Figure 3). Figure 4 is a reproduction from Forensic DNA typing by Butler [17] and the Quantifiler<sup>®</sup> Duo User's Manual [22] and depicts the mechanism just described.



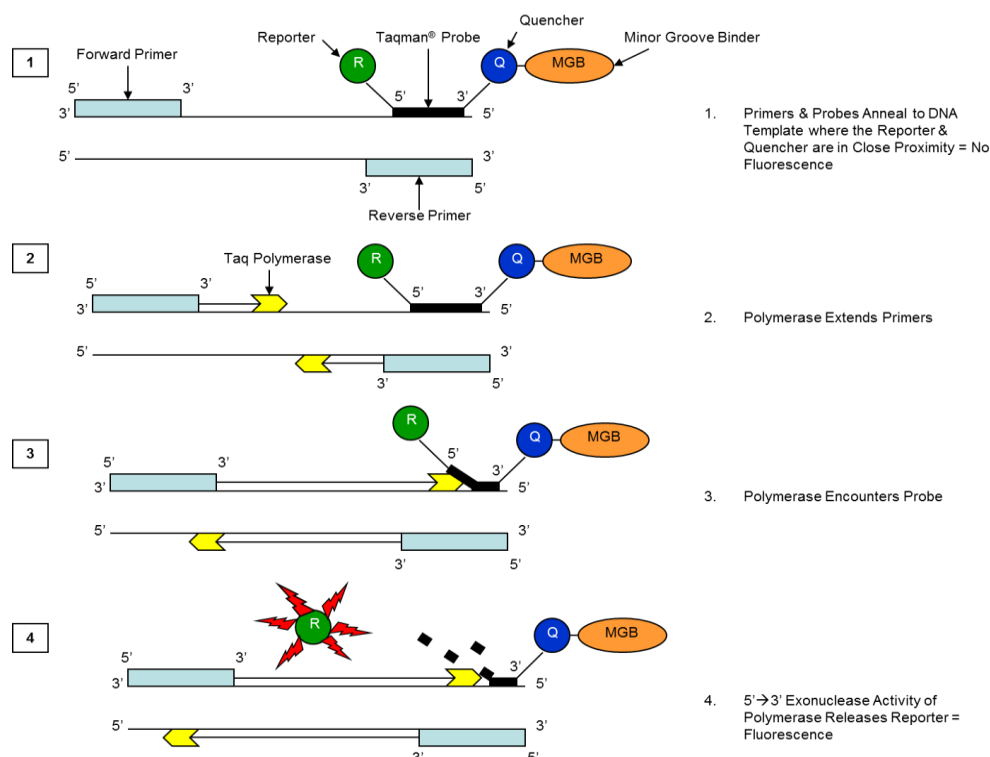


**Figure 4.** Illustration of the Taqman<sup>®</sup> probe detection method of real-time PCR.

Quantifiler<sup>®</sup> Duo is a multiplexed real-time quantification platform used to simultaneously determine total human and male DNA concentrations. It does this by monitoring the accumulation of two specific PCR products: a 140 base amplicon within the Ribonuclease P RNA Component H1 (RPPH1) gene for the determination of total human DNA and a 130 base amplicon within the Sex-determining Region Y (SRY) gene for the quantification of male DNA [22]. In real-time PCR, the signal output is measured in Cycle Threshold, or the cycle number at which fluorescence crosses a set threshold (0.2, as recommended by the manufacturer), and is referred to as the  $C_T$  value (Figure 3). If the amplification efficiency is 100%, the concentration of the amplicon is proportional to cycle number and the original concentration of template DNA according to

Equation 2. By taking the logarithm of both sides and defining N as the cycle threshold ( $C_T$ ), a direct proportionality between  $C_T$  and  $\log C_0$  is obtained:

$$\frac{\log C_N}{\log 2} - \frac{\log C_0}{\log 2} = C_T \quad (\text{Equation 3})$$

where the y-intercept is  $\frac{\log C_N}{\log 2}$  and the slope is  $-\frac{1}{\log 2}$  or -3.32. Therefore, a calibration curve can be established by running a series of standard DNA dilutions such that the  $C_T$  “signal” of an unknown can be compared to calibrators and unknown quantities estimated.

As previously described, the chemistries, analytes, and signal outputs of both methods (immunochromatographic test strips and real-time PCR) differ; furthermore, there is no known correlation between the amount of DNA and the amount of protein present in a given sample. Together, these factors make a direct signal comparison between systems impossible. Instead, the presence of matrix affects, sensitivity, limits of detection in terms of volume of body fluid, and reproducibility were evaluated to determine if one was a preferable screening method.

## Materials & Methods

All aspects of this study were conducted in compliance with ethical standards set forth by the Institutional Review Board of Boston University School of Medicine – Protocol H – 26187.

Unless otherwise noted, all reagents were purchased or supplied through Fisher Scientific (Fair Lawn, NJ).

### *Body Fluid Dilution Series*

The analyte detected, in all samples evaluated throughout the course of this study, was always a component of the male body fluid of interest. In order to determine if different matrices affected sensitivity, or the ability to detect this male component, multiple dilution series of either semen (Serological Research Institute, Richmond, CA) or male saliva (Serological Research Institute, Richmond, CA) diluted in either TE buffer (10 mM Tris/0.1 mM EDTA) or female blood were analyzed by both lateral flow immunochromatographic test strips (RSID™ Saliva or RSID™ Semen, Independent Forensics, Hillside, IL) and real-time PCR quantification (Quantifiler® Duo, Applied Biosystems, Carlsbad, CA).

Two sets of each of the four body fluid mixtures – male saliva diluted with female blood, male saliva diluted with TE buffer, semen diluted with female blood, and semen diluted with TE buffer – were prepared, for a total of eight body fluid mixtures. Each body fluid mixture was actually a dilution series consisting of 11 samples, ranging from neat to 1:1000 dilutions, and having a total volume of 100 µL. See Table 1 for a summary of the volumes utilized. Biological fluid volumes

were the means to directly compare the analytical thresholds, Limits of Detection (LOD), and sensitivities between the two methods due to the fact that the chemistries, analytes, and signal outputs of both systems differ, making a direct comparison between the concentration, or mass, of the analytes erroneous. Since the purpose of this study is to determine whether qPCR is a suitable replacement for the immunoassay cards, then qPCR would need to exhibit comparable or better figures of merit than the immunochromatographic test strips. Hence, the sensitivity and LODs, in terms of volume of body fluid of one individual, were evaluated to determine if one was a preferable screening method.

**Table 1.** List and preparation of the 11 samples in each body fluid dilution series. Values in parenthesis represent dilutions of the body fluid of interest prior to its addition to the mixture.

Dilution Number	Volume Ratio	Volume Semen or Saliva ( $\mu\text{L}$ )	Volume TE Buffer or Blood ( $\mu\text{L}$ )
1	Neat	100	0
2	1:2	50	50
3	1:5	20	80
4	1:10	10	90
5	1:20	5	95
6	1:50	2	98
7	1:100	1	99
8	1:250	4 (1:10)	96
9	1:500	2 (1:10)	98
10	1:750	1.33 (1:10)	98.67
11	1:1000	1 (1:10)	99

After mixture preparation, each of the 100  $\mu\text{L}$  samples was split into three replicates. To account for pipetting error, aliquots of 30  $\mu\text{L}$  were used. Later calculations are based on this 30  $\mu\text{L}$  total volume instead of a 100  $\mu\text{L}$  total

volume. Replicate aliquots were frozen at approximately  $-37^{\circ}\text{C}$  prior to extraction in order to preserve the biological material until use. See Figure 5 for a summary of body fluid dilution series preparation.

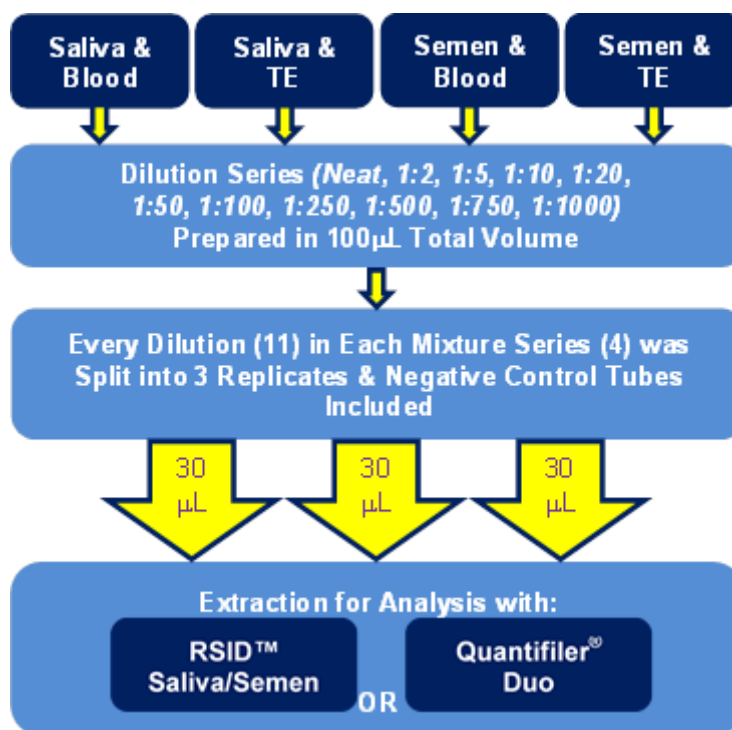


**Figure 5.** Flow chart of sample preparation for body fluid mixtures.

#### *Extraction for Amylase*

Replicate dilution series of either the male saliva diluted with female blood or the male saliva diluted with TE buffer were subjected to RSID™ Saliva lateral flow immunochromatographic test strips (Lot #041609A1, Independent Forensics, Hillside, IL) for the detection of salivary  $\alpha$ -amylase. To each tube containing the 30 µL aliquots of the dilution samples, 600 µL of RSID™ Saliva Extraction Buffer (Lot #031809EB, Independent Forensics, Hillside, IL) was added. Samples were agitated at room temperature on a mechanical shaker for

approximately 30 minutes prior to centrifugation for 3 minutes at 14,000 RPM. Following centrifugation, 20  $\mu\text{L}$  of supernatant was transferred to a second tube containing 80  $\mu\text{L}$  of RSID™ Saliva Running Buffer (Lot #031909SaRB, Independent Forensics, Hillside, IL). The entire 100  $\mu\text{L}$  extract-buffer mixture was pipetted onto the sample well of an RSID™ Saliva card, and per the manufacturer's suggested protocol, results were read after 10 minutes [23].

#### *Extraction for Sperm Cells and Semenogelin*

Semen sample extractions required preparation of microscope slides to detect sperm cells. To each tube containing the 30  $\mu\text{L}$  aliquots of the semen and blood or semen and TE dilution samples, 600  $\mu\text{L}$  saline (0.90 w/v, RICCA Chemicals, Arlington, TX) was added. Samples were agitated at room temperature on a mechanical shaker for approximately 30 minutes prior to centrifugation for 3 minutes at 14,000 RPM. Following centrifugation, 200  $\mu\text{L}$  of supernatant was transferred to a second microcentrifuge tube and set aside for further analysis.

To the initial sample tube, 170  $\mu\text{L}$  of TES (1 M pH8 Tris-HCl/0.5 M pH8 EDTA/20% w/v Sarkosyl, Sarkosyl from Teknova Science Matters, Hollister, CA) and 30  $\mu\text{L}$  of ProK (0.5 mg/mL) were added; samples were then incubated in a 37°C oven for two hours. Following incubation, samples were spun in a centrifuge for 3 minutes at 14,000 RPM to facilitate the formation of a sperm cell pellet at the bottom of the microcentrifuge tubes. After washing and resuspension of the sperm cell pellet with deionized water, the extracts (~15  $\mu\text{L}$ )

were heat fixed onto microscope slides, and stained with Hematoxylin (Harris Modified Hematoxylin with Acetic Acid) and Eosin (1% Eosin Y) to facilitate visualization of sperm cells. Sperm cell slides were then examined microscopically and qualitatively ranked on a 0 – 4 point scale: 0 = no sperm cells, 1 = hard to find (~20 cells), 2 = some sperm in many fields, 3 = some sperm in most fields, and 4 = many sperm in most fields. The arithmetic mean of the rankings was then calculated for later comparison.

From the microcentrifuge tubes that contained the 200  $\mu$ L of supernatant previously set aside, 20  $\mu$ L of supernatant was removed and added to new microcentrifuge tube containing 80  $\mu$ L of RSID™ Semen Running Buffer (Lot #RB030209, Independent Forensics, Hillside, IL). The entire 100  $\mu$ L extract-buffer mixture was then pipetted onto the sample well of an RSID™ Semen card (Lot #032409S1, Independent Forensics, Hillside, IL) for the detection of semenogelin, and per the manufacturer's suggested protocol, results were read after 10 minutes [15].

#### *Immunochromatographic Test Strips & ImageJ*

After running each sample on its respective RSID™ Saliva or RSID™ Semen card, the presence of a red band in the test region was interpreted visually by a single analyst, and each card was photographed. Due to the subjective nature of the visual inspection, the qualitative nature of the lateral flow immunochromatographic test strips, and the need to be able to compare the card output with the real-time PCR measurements, a method to assign numerical

values to the intensity of the red band in the test region of the cards was needed. ImageJ, free public NIH software that can process Java™ images, was utilized for this purpose. The Plot Profile function of ImageJ displays a graph of pixel intensity (measured in gray value) on the Y-axis versus distance (measured in pixels) on the X-axis [9]. In the case of the immunoassay cards, each line plot profile that is produced potentially contains two peaks, one representing the test band and one representing the control band, where there is an inverse relationship between gray value and analyte concentration (i.e. the higher the gray value the lower the analyte).

User-defined line profile plots were created for each immunoassay card from the compatible digital photographs (i.e. JPEG) taken at the time of testing. The image of interest was selected and the ImageJ “Straight, Segmented, Freehand Line and Arrow Tool” was employed to trace a line over the area to be analyzed by the software, in this case, the test well of each immunoassay card. Special care was taken to ensure that the line was drawn in the same orientation every time. Therefore, it was arbitrarily decided that the zero point of each graph would represent the end of the test well that was closest to the sample well resulting in a plot profile with two peaks, the one closest to the zero point representing the test band and the second peak representing the control band. A list of the data points from each graph, which were comprised of pixel intensity versus distance, was saved in .xls format for further statistical and analytical evaluation using Microsoft® Excel® 2010 and its Data Analysis ToolPak®



(Redmond, WA). In assessing the maximum gray scale intensity, the single point of interest for each plot profile graph was the apex of each sample peak, which was taken to be the data point that represented the peak minimum.

#### *Organic Extraction of DNA*

All four types of body fluid mixture dilution series were organically extracted using the same procedure, regardless of whether the component of interest was semen or male saliva. For the organic extraction lysis, the following reagents were added to each 30  $\mu$ L dilution series aliquot tube and negative control: 150  $\mu$ L TEN (10 mM Tris/1 mM EDTA/100 mM NaCl, NaCl from Acros Organics via Fisher, Fair Lawn, NJ), 50  $\mu$ L Sarkosyl (20% w/v, Teknova Science Matters, Hollister, CA), 15  $\mu$ L DTT (1 M, Acros Organics via Fisher, Fair Lawn, NJ), 165  $\mu$ L distilled water (Millipore, Billerica, MA), and 20  $\mu$ L ProK (10 mg/mL), for a total volume of 430  $\mu$ L per tube. All samples were then incubated at 37°C for eighteen hours.

After incubation, an equal volume (430  $\mu$ L) of Phenol/Chloroform/Isoamyl alcohol (PCI) was added to each sample tube, and the tubes were shaken by inversion. To separate the organic layer from the aqueous layer, each tube was centrifuged for 3 minutes at 12,000 RPM. After centrifugation, the aqueous layer was transferred to an assembled microcon filter (Millipore, Billerica, MA) and tube. Note, only 80% (344  $\mu$ L) of the aqueous layer was transferred from each sample to ensure a consistent total volume between samples. Each microcon assembly was centrifuged at 2,400 RPM for 15 minutes, and the filtrate

discarded. A volume of 400  $\mu\text{L}$  of TE buffer was added to each concentrator, and the assemblies were then centrifuged at 2,400 RPM for 20 minutes. Additional spin times, either 30 or 35 minutes, were necessary to remove excess filtrate. To recover the DNA from the microcon column, an additional 10  $\mu\text{L}$  of TE buffer was added to the filter before it was inverted into a second tube. The filter and recovery tube assembly were centrifuged at 3,500 RPM for 5 minutes. Eluents were transferred to screw cap microcentrifuge tubes for storage and brought up to a final volume of 25  $\mu\text{L}$  with TE buffer.

#### *Real-Time PCR*

Aliquots of each body fluid mixture dilution sample organically extracted for DNA were subjected to real-time PRC quantification in a 96-well microtiter plate format, on an Applied Biosystems Prism<sup>®</sup> 7500 Sequence Detection System (Applied Biosystems, Carlsbad, CA), with the dual human and male Quantifiler<sup>®</sup> Duo platform (Applied Biosystems, Carlsbad, CA), under 9600 emulation conditions per the manufacture's protocol [22]. A three-fold dilution series with eight concentration points, ranging from 50 ng/ $\mu\text{L}$  to 0.023 ng/ $\mu\text{L}$ , was run in duplicate on each plate to produce the standard curve per the manufacturer's protocol [22], except that an outside source of stock DNA was used to prepare the real-time PCR standard dilution series [24]. The series was created by first diluting human genomic male DNA (251 ng/ $\mu\text{L}$ , Promega, Madison, WI) to 22.95 ng/ $\mu\text{L}$  by adding 545.14  $\mu\text{L}$  of Tris-EDTA Glycogen buffer (TEG) to 54.86  $\mu\text{L}$  of the stock DNA (10 mM Tris/0.1 mM EDTA/20 mg/mL

Glycogen). Successive points in the series were created by diluting 150  $\mu\text{L}$  of the previous sample with 300  $\mu\text{L}$  of TEG. Aliquots of the standard dilution series were frozen at  $-37^{\circ}\text{C}$  until use.

A master mix composed of the Quantifiler<sup>®</sup> Duo Primer Mix (10.5  $\mu\text{L}$  per sample) and the Quantifiler<sup>®</sup> Duo Reaction Mix (12.5  $\mu\text{L}$  per sample) was created for each plate and 23  $\mu\text{L}$  of master mix was dispensed into the appropriate wells, according to the plate record. A volume of 2  $\mu\text{L}$  of each standard, control, and sample was dispensed into the assigned wells for a total reaction volume of 25  $\mu\text{L}$ . In this study, only the male-specific  $C_T$  values were used to determine the real-time PCR's analytical figures of merit, which were directly compared to those derived from the immunoassay cards.

## Results & Discussion

### *Raw Data*

As previously mentioned, the analytes being measured and the signal outputs for both analytical methods, lateral flow immunochromatographic test strips and real-time PCR, differ. What is actually being interpreted with the immunoassay cards is a red band in the test region of the cassette, which represents a positive test result for the presence of the analyte of interest. Figure 6A displays the results of the third replicate of the saliva-TE dilution series run on the RSID™ Saliva cards, which detect the presence of the human salivary  $\alpha$ -amylase antigen, and Figure 6B displays the results of the third replicate of the semen-blood dilution series run on the RSID™ Semen cards, which detect the presence of human semenogelin antigen. Qualitatively, it is observed that the control band at the top of each test well is visible, demonstrating that the cards were functioning properly. The result for each sample is indicated by the presence or absence of a red band at the bottom of each test strip. The semi-quantitative nature of the immunoassay cards is apparent by visually comparing the relative intensity of each of the test bands.



**Figure 6.** (A) Third replicate of the saliva-TE dilution series run on RSID™ Saliva lateral flow immunochromatographic test strips. (B) Third replicate of the semen-blood dilution series run on RSID™ Semen lateral flow immunochromatographic test strips.

To assign a numeric value to the intensity of the test band for each test strip, the JPEG images were analyzed using the Plot Profile function of ImageJ. The data output of this modality is a graph of gray value intensity verse distance, an example of which is shown in Figure 7. From the plot profile graphs, the sample peak always fell between 200 and 400 pixels while the control peak fell between 400 and 700. The peak minimum of the test band in each plot profile graph was taken to represent the signal for that corresponding immunoassay card.

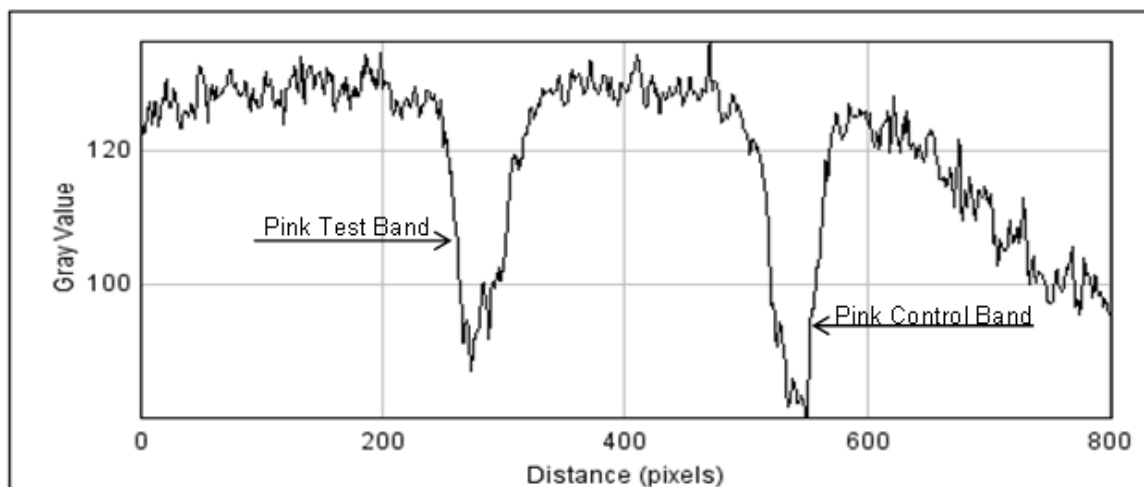


**Figure 7.** ImageJ software output for the third replicate of the semen-blood 1:50 dilution (immunoassay card seen in Figure 6).

Traditionally in forensics, immunochromatographic test strips have been suggested to be qualitative and are not commonly used to determine the quantity of analyte. This may be due to the high degree of variability of the levels of  $\alpha$ -amylase and semenogelin from person-to-person [25-27] and the variability in the recovery and persistence of these enzymes [28-30], thereby rendering absolute quantification difficult. However, semi-quantitative analysis using the test strips and image processing software has previously been performed. Specifically, Tian et al. [31] tested urine for the presence of nortestosterone, an exogenous anabolic steroid, with immunochromatographic test strips. Using ImageJ software to calculate optical density (OD) values from digital images of the test strips, they found there was a dose-response between nortestosterone concentration and optical density [31]. Additionally, Zhao et al. [12] tested the ability of DNase I to generate a color change by exploiting gold nanoparticle aggregation and dispersion states. They acknowledge that these types of

assays are generally used to provide qualitative information, but state that it is possible to obtain quantitative information through the use of image processing software, such as ImageJ [12]. This suggests that for purposes of method comparison, using volumes of body fluid originating from one individual as was done in this study, semi-quantitative analysis of immunoassay cards via ImageJ is appropriate.

As previously described, the more analyte that is present in the sample, the darker the red band in the test region and the lower the gray value when plotted in ImageJ due to the inverse nature of the graphical representation. For most samples, this was observed as seen in Figure 9A. The exception to this was observed in semen samples tested on RSID™ Semen cards (Figure 9B). This figure shows that as the volume of semen increases, the gray value increases, representing a signal decrease on the card. This phenomenon is attributed to the High-Dose Hook Effect, which has previously been characterized and is attributed to high levels of target antigen in the test sample [32, 33]. The high-dose hook effect occurs when the amount of target antigen in the sample is sufficient to result in a significant amount of target antigen remaining unbound to the colloidal gold-labeled antibody. Free antigen is then expected to migrate ahead of the labeled antibody-antigen complexes, thereby occupying the bound antibody on the test line with unlabeled antigen and decreasing the number of sites for the gold-labeled antibody-antigen complexes [32]. Evidence of the high-dose hook effect can be seen in Figure 6B, with the RSID™ Semen cards, where

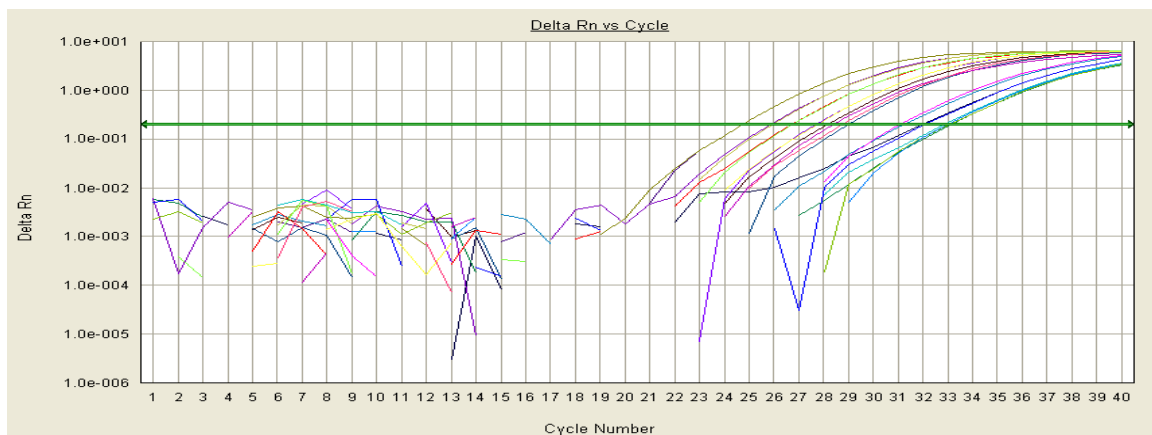
it was observed that the most intense signals were seen when the semen sample was diluted by 20-100 times the volume of blood. Less dilute samples and neat semen exhibited sample intensities similar to very dilute samples (i.e. 1:750). This is in contrast to the RSID™ Saliva cards (Figure 6A). The high-dose hook effect was observed for all semen dilution series but only seemed to affect the neat saliva samples (Figure 9). This finding is consistent with the manufacturer's developmental validations where no evidence of the high-dose hook effect using the RSID™ Saliva cards was observed, but the RSID™ Semen cards demonstrated the effect with samples containing the equivalent of 3  $\mu$ L or greater of semen [32, 33].

Notably, the high-dose hook effect has been utilized as a mode of detection aiding in establishing whether an analyte is present above an acceptable threshold [31, 34, 35]. For example, Tian et al. use the high-dose hook effect to screen livestock, making sure nortestosterone does not exceed regulated limits. In the field of forensics, however, it is more common to deal with samples that contain low levels of the body fluid of interest rather than those that have an abundant amount, so the influence of the high-dose hook effect may be negligible. Nevertheless, when attempting to identify semen on an item of evidence, the two test approach, which utilizes both microscopic sperm searches followed by immunochromatographic test strips when no sperm are observed, is commonly employed by forensic laboratories. Therefore, although the high-dose hook effect may lead to a false negative when testing for semenogelin via



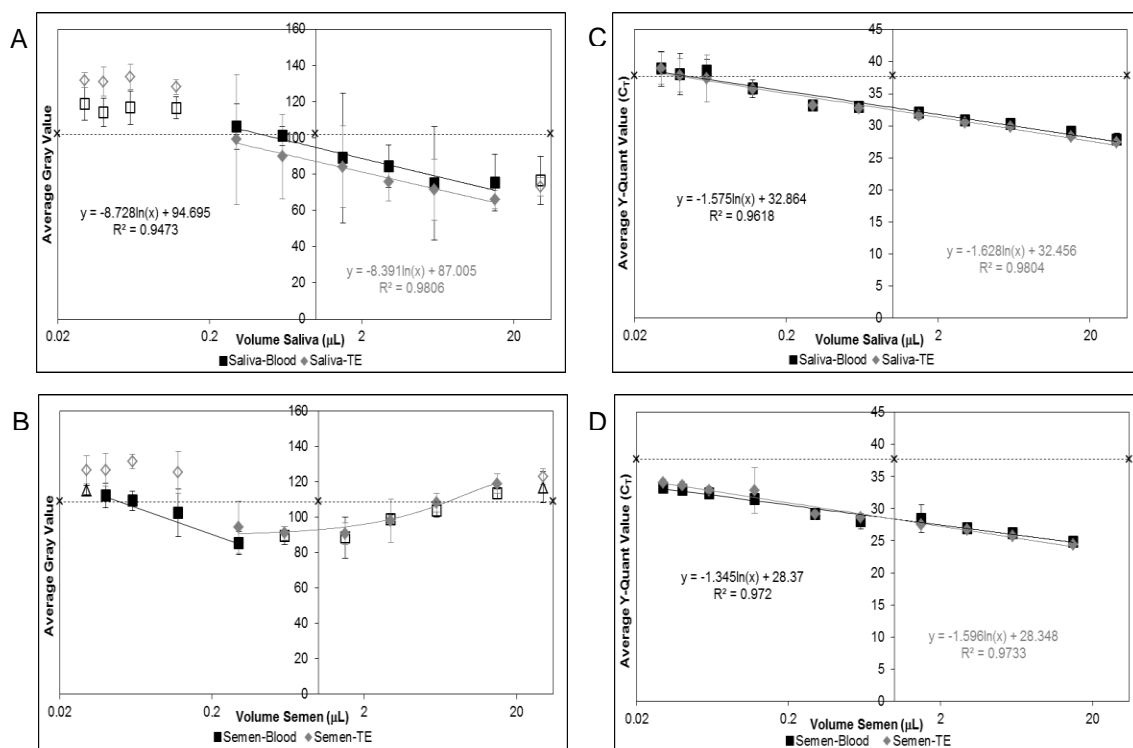
immunoassay cards, high volumes of semen which have not been diluted to a significant extent are still expected to result in observable sperm during microscopic evaluation. This helps to ensure that the probability of a sample being falsely characterized as containing no typable DNA material remains low. Therefore, for laboratories that rely solely on immunochromatographic screening tests, a second test (i.e. microscopic sperm searches) is recommended for samples that are expected to contain highly concentrated semen.

Figure 8 displays the amplification plots for the third replicate of the semen-blood dilution series run on an Applied Biosystems 7500 instrument; this is the real-time PCR signal output for samples displayed in Figure 6B. Note, as with the immunochromatographic test strips, there is an inverse relationship between  $C_T$  value and concentration, with samples having a higher concentration of analyte crossing the analysis threshold at earlier cycle numbers than samples with a lower concentration of analyte.



**Figure 8.** Real-time PCR amplification plots for the third replicate of the semen-blood dilution series. The horizontal green line represents the signal intensity threshold needed for the  $C_T$  to be recorded.

Figure 9 consists of four graphs displaying the relationship between signal and sample volume for the immunochromatographic test strips and the real-time PCR platforms. Data points represent the average value of the signal outputs – gray scale intensity or  $C_T$  value – for the three replicates of each dilution in the series, and all error bars represent two standard deviations about the mean. As previously stated, volume ( $\mu\text{L}$ ) was chosen as the means of comparison between methods because the chemistries, analytes, and signal outputs differ. Figure 9 shows that the relationship between signal and volume is log-linear with all  $R^2$  values being greater than or equal to 0.95, which suggests for Figures 9A, 9C, and 9D, the signal decreases with increasing volume in a definable way. This log-volume-to-signal relationship can, therefore, be exploited as the basis to derive analytical figures of merit typically used in analytical, physical, and environmental chemistry.



**Figure 9.** Sensitivity curves for immunochromatographic test strips and real-time PCR quantification platforms. (A) Saliva-Blood and Saliva-TE dilution series on RSID™ Saliva cards, (B) Semen-Blood and Semen-TE dilution series on RSID™ Semen cards, (C) Saliva-Blood and Saliva-TE dilution series with Quantifiler® Duo, and (D) Semen-Blood and Semen-TE dilution series with Quantifiler® Duo.

The dashed horizontal lines in Figure 9 represent one such figure of merit, the Minimum Distinguishable Signal (MDS), which is defined as the lowest analytical output that can be separated from the baseline noise for a given platform [36], and which was developed by Kaiser [37, 38]. The MDSs of the immunoassay cards were determined for each sample by calculating the mean signal of the corresponding blanks (MBS) and subtracting three standard deviations. See Table 2 for immunoassay card MDS values that correspond to the lines shown in Figures 9A and 9B. As seen by Figure 9, the MDS as calculated with quantitative analysis of the image suggests it is an appropriate

metric because signal below the MDS (i.e. above the line) does not increase with volume, suggesting the MDS calculated via Kaiser's [37, 38] method is representative of signal which cannot easily be distinguished from baseline. This can be qualitatively observed in Figure 6 where it becomes difficult to see the red bands in the test region as volume of body fluid decreases.

**Table 2.** Immunoassay card MBS and standard deviation values used to calculate MDS values (shown in bold), which are plotted as dashed horizontal lines in Figures 9A (saliva-blood and saliva-TE) and 9B (semen-blood and semen-TE) and later in Figures 11A (saliva) and 11B (semen).

Body Fluid	MBS (Gray Value)	Standard Deviation	MDS (Gray Value)
Saliva	125.4	7.8	<b>102.0</b>
Semen	124.9	5.4	<b>108.6</b>

A number of unfilled points exist on the immunoassay card graphs in Figures 9A and 9B that were not included in their respective trendlines. These unfilled points are meant to represent one of two things: 1) results that were less than the dilution series' MDS or 2) samples affected by the high-dose hook effect and, therefore, were not used to calculate the linear parameters and their subsequent errors. Both types of points are unreliable measures of analyte concentration because they fall outside of the cards' linear range. In Figure 9A, the four points in both the saliva-blood and saliva-TE series that correspond to the 1:250, 1:500, 1:750, and 1:1000 dilutions were excluded because they were less than their respective MDS values. Furthermore, the neat saliva samples for both series were excluded due to the high-dose hook effect. The semen-blood dilution series of Figure 9B had two unfilled points (neat and 1:1000) that were

less than the MDS, and the remainder of the unfilled points (1:2, 1:5, 1:10, 1:20, and 1:50) were excluded due to the high-dose hook effect. Also in Figure 9B, all of the unfilled points in the semen-TE dilution series (neat, 1:250, 1:500, 1:750, and 1:1000) were less than the MDS. Additionally, the results for the neat semen samples are not included in Figure 9D due to detected concentrations outside the dynamic range of the system, as was defined by concentrations that exceeded 100 ng/ $\mu$ L [39, 40].

Because the signal output is measured in cycle threshold ( $C_T$ ), or the cycle number at which fluorescence crosses a set threshold of 0.20 [22], the approach to determine the MDS values for the Quantifiler<sup>®</sup> Duo platform (Figures 9C & 9D) cannot rely on the MBS. That is, since there is no template DNA to amplify in a blank sample, there will be no increase in fluorescence, resulting in a real-time PCR  $C_T$  value which will always be undetermined. As a result, a different approach for defining the MDS, one that depends on the standard curve, was applied. If extrapolation from the standard curve is *not* used in order to determine the concentration of a low level unknown, then the mean male  $C_T$  value of the 0.023 ng (point “H”) calibration standard (36.00  $C_T$ ) minus three standard deviations (2.25) can be used as the MDS (33.75  $C_T$ ). If the concentration of a low level unknown *is* extrapolated from the standard curve, a  $C_T$  equal to 40 – the highest  $C_T$  value that the Quantifiler<sup>®</sup> Duo platform is set to detect – can also be used as the MBS. The standard deviation of the 40  $C_T$  MBS was estimated by modeling the errors for each of the eight points in the real-time

PCR standard curves. Figure 10 shows that the  $C_T$ 's error increases with decreasing volume. If the relationship is approximated as linear, by substituting the  $C_T$  of 40 into the trendline equation shown in Figure 10, an error of 0.7732 can be approximated for the real-time PCR MBS of 40  $C_T$ . There are limitations, however, to this method due to the fact that the model shown in Figure 10 is not perfectly linear, as evidenced by an  $R^2$  of 0.7969, and may actually be exponential in nature. Though more work needs to be conducted in this area to better estimate the error of the 40  $C_T$  MBS, the linear approximation was used to simplify the determination of the associated error, and the 40  $C_T$  MBS minus three standard deviations (2.32) was used as the MDS (37.68  $C_T$ ). Therefore, depending on the laboratory's protocol, either 33.75  $C_T$  or 37.68  $C_T$  could be considered the MDS. A line representing only the MDS equal to a  $C_T$  of 37.68 is shown in Figures 9C and 9D due to the stochastic nature of the measurement at the low end of the standard curve.

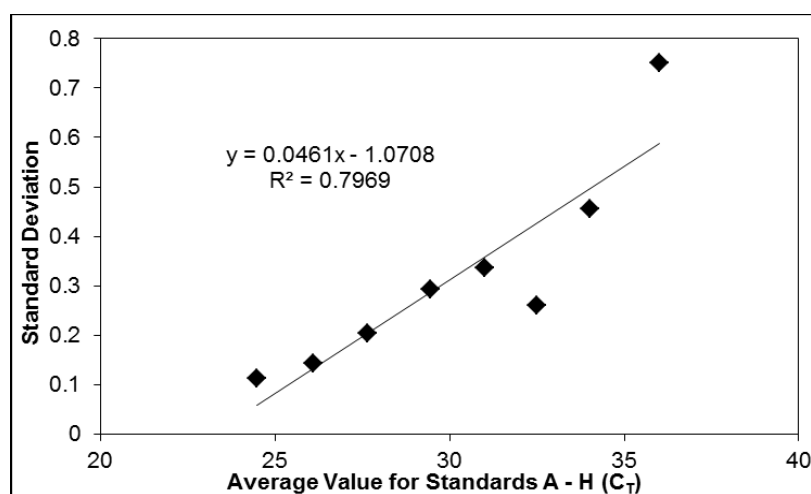


**Figure 10.** Determination of error for the 40  $C_T$  MBS by modeling the errors of the 8 points (A – H) in the real-time PCR standard curve.

### *Matrix Effects and Sensitivity*

Sensitivity is one way to describe the performance of an instrument or method, but is often confused with the Limit of Detection (LOD), when, in fact, the two terms have related but unique analytical meanings. An instrument's or method's sensitivity is used to describe minute changes in signal with respect to changes in mass or concentration [36]. The simplest definition of sensitivity is the change in signal per unit change in analyte concentration. If this change is constant over a wide mass range, the term is mathematically the same as the slope of a straight line with the equation:

$$y = mc + b \quad \text{(Equation 4)}$$

where  $y$  is the measured signal,  $c$  is the concentration or mass of the analyte,  $b$  is the y-intercept, and  $m$  is the slope [36]. The above description is consistent with the International Union of Pure and Applied Chemistry (IUPAC) definition of sensitivity, which is the slope of the calibration curve at the concentration of interest [41] and is referred to as calibration sensitivity. When calibration sensitivity is used to compare two systems, the calibration curve with the steeper slope is deemed more sensitive [36].

Since the calibration sensitivities are represented by the slope, a least-squares linear regression results in both the slope and the error of the slope as seen in Table 3. No trendline equation is given for the semen-blood or semen-TE immunoassay card dilution series (Figure 9B) because neither relationship is defined by a log-linear one.

**Table 3.** Calibration sensitivities for body fluid dilution series analyzed with RSID™ Saliva cards, RSID™ Semen cards, and Quantifiler® Duo.

Body Fluid Mixture	RSID™ Card Calibration Sensitivity	Quantifiler® Duo Calibration Sensitivity
Saliva-Blood	-8.73 (+/- 1.03)	-1.58 (+/- 0.11)
Saliva-TE	-8.39 (+/- 0.59)	-1.63 (+/- 0.08)
Semen-Blood	---	-1.35 (+/- 0.08)
Semen-TE	---	-1.60 (+/- 0.09)

From Table 3, slopes between samples diluted with blood and TE do not differ significantly indicating there is no significant matrix effects using either analysis platform. This lack of matrix effects is also illustrated by overlapping error bars between samples diluted with blood and TE as seen in Figure 9. From Table 3, it is also observed that the slopes of the calibration curves are larger for the immunochromatographic test strips than for real-time PCR, which would seem to indicate that the immunoassay cards are more sensitive to changes in analyte concentration than real-time PCR. However, this is only the case if one fails to take into account the precision of the measurements, which is done through the use of analytical sensitivities and the equation:

$$\gamma = m/s \quad (\text{Equation 5})$$

where  $\gamma$  is the analytical sensitivity,  $m$  is the slope of the calibration curve (or the calibration sensitivity), and  $s$  is the standard deviation of the measurement [36]. Refer to Tables 4 – 7 for a complete listing of analytical sensitivities.



**Table 4.** Analytical sensitivities for Saliva-Blood dilution series  
analyzed with RSID™ Saliva cards and Quantifiler® Duo.

Volume Ratio (Saliva-Blood)	RSID™ Saliva Cards		Quantifiler® Duo	
	Standard Deviation	Analytical Sensitivity	Standard Deviation	Analytical Sensitivity
Neat	6.62	-1.32	0.49	-3.23
1:2	7.85	-1.11	0.21	-7.59
1:5	15.6	-0.56	0.21	-7.65
1:10	5.89	-1.48	0.28	-5.67
1:20	17.9	-0.49	0.20	-7.72
1:50	2.68	-3.26	0.29	-5.46
1:100	6.28	-1.39	0.21	-7.65
1:250	2.97	-2.94	0.72	-2.20
1:500	4.61	-1.89	0.85	-1.85
1:750	3.91	-2.23	1.62	-0.97
1:1000	4.54	-1.92	1.38	-1.15

**Table 5.** Analytical sensitivities for Saliva-TE dilution series  
analyzed with RSID™ Saliva cards and Quantifiler® Duo.

Volume Ratio (Saliva-TE)	RSID™ Saliva Cards		Quantifiler® Duo	
	Standard Deviation	Analytical Sensitivity	Standard Deviation	Analytical Sensitivity
Neat	2.55	-3.29	0.19	-8.40
1:2	8.42	-1.00	0.08	-19.6
1:5	5.28	-1.59	0.17	-9.80
1:10	11.2	-0.75	0.26	-6.25
1:20	11.7	-0.72	0.37	-4.45
1:50	17.9	-0.47	0.18	-9.08
1:100	21.7	-0.39	0.29	-5.64
1:250	2.01	-4.18	0.47	-3.49
1:500	3.52	-2.39	1.83	-0.89
1:750	3.95	-2.12	1.32	-1.24
1:1000	1.98	-4.23	1.24	-1.31

**Table 6.** Analytical sensitivities for Semen-Blood dilution series analyzed with RSID™ Semen cards and Quantifiler® Duo.

Volume Ratio (Semen-Blood)	RSID™ Semen Cards		Quantifiler® Duo	
	Standard Deviation	Analytical Sensitivity	Standard Deviation	Analytical Sensitivity
Neat	4.32	---	0.25	-5.33
1:2	1.37	---	0.20	-6.67
1:5	1.71	---	0.24	-5.62
1:10	1.20	---	0.27	-4.96
1:20	5.82	---	1.08	-1.25
1:50	2.46	---	0.62	-2.16
1:100	3.27	---	0.40	-3.40
1:250	6.68	---	0.37	-3.62
1:500	2.73	---	0.26	-5.22
1:750	3.39	---	0.15	-8.74
1:1000	1.29	---	0.31	-4.31

**Table 7.** Analytical sensitivities for Semen-TE dilution series analyzed with RSID™ Semen cards and Quantifiler® Duo.

Volume Ratio (Semen-TE)	RSID™ Semen Cards		Quantifiler® Duo	
	Standard Deviation	Analytical Sensitivity	Standard Deviation	Analytical Sensitivity
Neat	2.28	---	2.40	-0.67
1:2	2.75	---	0.22	-7.36
1:5	2.57	---	0.14	-11.5
1:10	6.13	---	0.18	-8.82
1:20	3.14	---	0.17	-9.53
1:50	1.95	---	0.36	-4.38
1:100	7.35	---	0.35	-4.53
1:250	5.93	---	1.77	-0.90
1:500	2.00	---	0.31	-5.08
1:750	4.54	---	0.36	-4.37
1:1000	4.02	---	0.27	-5.96

To explain how factoring in the standard deviation alters the sensitivity, the values in Table 4 will be used as an example. When comparing the standard deviations of the RSID™ Saliva card measurements with those of the Quantifiler® Duo measurements, it is observed that the standard deviations for Quantifiler®

Duo are a minimum of 2.4 and a maximum of 89.5 times smaller than those of the RSID™ Saliva cards, which suggests that the immunoassay card measurements are less precise than real-time PCR. Looking at the standard deviations for each method independently, two separate models emerge. The RSID™ Saliva card standard deviation varies considerably from dilution to dilution: from the 1:2 to the 1:5, there is an approximate doubling, which is followed by a roughly three-fold decrease, a three-fold increase, then a six-fold decrease. The Quantifiler® Duo standard deviation, on the other hand, stays consistent until the 1:250 dilution, where it increases by just over a factor of three, then doubles at the 1:750 dilution. While there appears to be no pattern to the immunoassay card standard deviation, the increase in standard deviation seen with Quantifiler® Duo is consistent with stochastic effects known to exist when amplifying small quantities of DNA [42]. It is worth noting that when the Quantifiler® Duo standard deviations are compared between saliva and semen dilution series, stochastic effects have less of an impact on the semen samples, presumably because semen contains more genetic material than saliva, as seen by the smaller  $C_T$  values at an equivalent volume (Figures 9C & 9D).

As with calibration sensitivity, higher analytical sensitivity values indicate a greater signal change with changes in analyte concentration. In Table 4, the analytical sensitivity values are consistently larger with real-time PCR than with immunoassay cards until the 1:250 dilution, where the analytical sensitivities between the methods are roughly equivalent for the rest of the dilutions but

slightly higher for the RSID™ Saliva cards. This finding is consistent with the saliva-TE dilutions seen in Table 5. The analytical sensitivities for the RSID™ Semen cards are not given in Table 6 because the calibration sensitivity was derived from a linear, not a logarithmic, equation. Therefore, the analytical sensitivities of the semen-blood dilutions in Tables 6 are not directly comparable between the immunoassay cards and real-time PCR. The same is true for the semen-TE dilutions in Table 7, which have no analytical sensitivities associated with the RSID™ Semen cards due to the fact that a calibration sensitivity figure could not be generated. From Tables 4 – 7, there is again no indication of matrix effects illustrated using either analysis platform.

Because the different sample matrices (blood and TE) did not affect the detection of the body fluid of interest on either platform, data from the respective body fluid dilution series was combined, which allowed the overall calibration sensitivities for the two methods to be plotted against each other (Figure 11). Data points in the calibration curves depicted in Figure 11 represent the average value of the signal outputs for each dilution of either all saliva or all semen samples analyzed on a given platform, error bars are equivalent to two standard deviations, dashed horizontal lines correspond to MDS values, and unfilled points were not included in trendlines because they signify results that were less than the MDS or high-dose hook effect samples and , therefore, fell outside the linear range. For immunoassay card MBS and MDS values, refer to Table 2. Since Quantifiler® Duo MDS values are based on how the standard curve is applied,

they remained either 33.75  $C_T$  or 37.68  $C_T$ , but only the MDS corresponding to a  $C_T$  of 37.68 is plotted in Figures 11A and 11B.

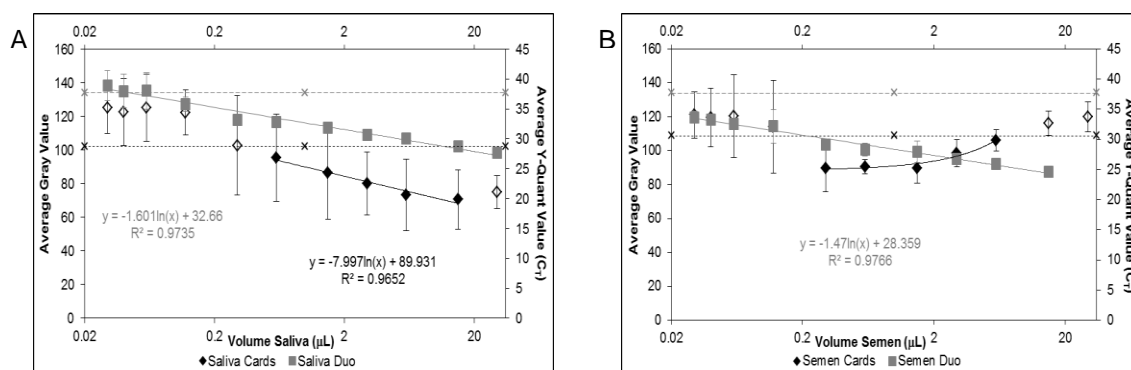


**Figure 11.** *RSID™ immunoassay card calibration sensitivity plotted against Quantifiler® Duo calibration sensitivity. (A) Overall Saliva and (B) Overall Semen.*

Trendlines with correlation coefficients ( $R^2$ ) greater than or equal to 0.95 were fit to the combined calibration sensitivity data. With the exception of the RSID™ Semen cards, on which the high-dose hook effect had a pronounced influence, the equations for each of these trendlines are displayed on the plots in Figure 11. Again, the RSID™ Semen card data is precluded from further characterization due to high-dose hook effect. For reference, the overall calibration sensitivities for each platform, which are equal to the slopes of the trendlines, are supplied in Table 8.

**Table 8.** *Overall calibration sensitivities for RSID™ Saliva cards, RSID™ Semen cards, and Quantifiler® Duo.*

Platform	Overall Calibration Sensitivity
RSID™ Saliva Cards	-8.00 Intensity/ $\mu$ L
Quantifiler® Duo (Saliva)	-1.60 $C_T$ / $\mu$ L
RSID™ Semen Cards	---
Quantifiler® Duo (Semen)	-1.47 $C_T$ / $\mu$ L

### *Overall Limits of Detection*

Sensitivity was defined previously as the change in signal per unit change in analyte concentration. In contrast, the Limit of Detection (LOD) is the input amount, volume of the body fluid of interest for example, that gives a signal significantly different from the blanks [43]. When attempting to quantify the minimum amount of analyte a system can detect, the LOD should not be used interchangeably with sensitivity. LODs were chosen as an absolute means of comparison between the RSID™ immunoassay cards and real-time PCR using Quantifiler® Duo chemistry.

Prior to numerical analysis, a visual inspection of the results shown in Figure 6 can provide insight with respect to MDS. Tables 9 and 10 summarize this by assigning a (+) sign to a positive result for the signal detection of a specific body fluid and a (-) sign to a negative result. In addition to ImageJ analysis of the RSID™ immunoassay cards and real-time PCR using Quantifiler® Duo, two additional means of evaluating the data were considered. In columns titled “Analyst’s Visual Inspection of Cards” that appear in both Tables 9 and 10, the presence or absence of a red band in the test region of each immunoassay card was interpreted visually by a single analyst. Another column titled “Average Sperm Cell Ranking” appears in only Table 10, and provides the results of the microscopic examination of sperm cell pellets obtained after extraction for semenogelin. For a specific dilution to be deemed positive in the visual inspection, ImageJ, or Quantifiler® Duo columns, at least half of the replicates

had to be interpreted as positive or produce a signal above the MDS.

Conversely, numeric scores are presented in the average sperm cell ranking column, as described in the Materials and Methods section. The arithmetic mean of the rankings was calculated and is the number presented in Table 10; an asterisk next to the ranking indicates that sperm cells were observed in five out of six slide preparations for that dilution.

**Table 9.** *Presence of signal – either a red band in the test region for immunoassay cards or a  $C_T$  value for real-time PCR – in detection of Saliva.*

Dilution	Volume Saliva ( $\mu$ L)	Overall Saliva		
		Analyst's Visual Inspection of Cards	ImageJ	Duo
Neat	30	+	+	+
1:2	15	+	+	+
1:5	6	+	+	+
1:10	3	+	+	+
1:20	1.5	+	+	+
1:50	0.6	+	+	+
1:100	0.3	+	-	+
1:250	0.12	+	-	+
1:500	0.06	-	-	+
1:750	0.04	-	-	+
1:1000	0.03	-	-	+

**Table 10.** Presence of signal – a red band in the test region for immunoassay cards, sperm on microscope slides, or a  $C_T$  value for real-time PCR – in detection of Semen.

Dilution	Volume Semen ( $\mu$ L)	Overall Semen			
		Analyst's Visual Inspection of Cards	Average Sperm Cell Ranking	ImageJ	Duo
Neat	30	+	4	-	+
1:2	15	+	3.8	-	+
1:5	6	+	4	+	+
1:10	3	+	4	+	+
1:20	1.5	+	3.7	+	+
1:50	0.6	+	2.7	+	+
1:100	0.3	+	2.5	+	+
1:250	0.12	+	1.2*	-	+
1:500	0.06	-	1*	-	+
1:750	0.04	-	0.8*	-	+
1:1000	0.03	-	1	-	+

By comparing results across methods, a picture of the relative MDSs begins to emerge. Quantifiler<sup>®</sup> Duo was the only detection method to yield a positive result for every dilution of both the saliva (Table 9) and semen (Table 10) samples. The analysis depicted above estimates that the LOD of saliva and the LOD of semen on the Quantifiler<sup>®</sup> Duo platform should be around 0.03  $\mu$ L of body fluid. The average sperm cell rankings also netted a result for every dilution but only apply to the semen samples. Interestingly, the average sperm cell rankings drop considerably from the 1:100 dilution to the 1:250 dilution and beyond, and some slide preparations even generated negative results while Quantifiler<sup>®</sup> Duo with a MBS of 40  $C_T$  always resulted in signal. This demonstrates that with low amounts of input material, despite extensive mixing during sample preparation, there is a stochastic range when it comes to recovery of sperm cells after extraction. Furthermore, Quantifiler<sup>®</sup> Duo could be deemed



to have a lower Limit of Detection than the microscopic sperm cell checks because it would even detect lysed sperm cells or male epithelial cells when the microscopic screening would be considered negative.

When the two detection methods for the lateral flow immunochromatographic test strips are compared, the analyst's visual inspection of the immunoassay cards seems to have a lower LOD than the ImageJ analysis. For the saliva samples, when evaluating the same immunoassay cards, the human reader registered positive results down to the 1:250 dilution ( $\sim 0.12 \mu\text{L}$  of saliva) while the automated technique scored positive results down to the 1:50 dilution ( $\sim 0.6 \mu\text{L}$  of saliva). For the RSID™ Semen cards, the apparent LODs of the two interpretation schemes were closer, with the analyst indicating positive results down to the 1:250 dilution ( $\sim 0.12 \mu\text{L}$  of semen) and ImageJ down to the 1:100 dilution ( $\sim 0.3 \mu\text{L}$  of semen); however, with the concentrated semen samples, both were impacted by the high-dose hook effect. These findings seem unexpected until one takes into account the fact that the ImageJ results incorporate a noise threshold, in the form of the MDS, which the visual inspection does not. Additionally, ImageJ analysis is directly affected by the quality of the photographs and the lighting applied during data acquisition, and also by optimization of contrast and brightness during data analysis. Optimization of photograph acquisition may improve contrast and therefore result in a lower LOD and/or higher sensitivity.

While the visual assessment of the results displayed in Tables 9 and 10 can provide approximations of LODs for the various detection methods, a more rigorous approach for quantitatively determining the LODs is needed to make a meaningful comparison. By substituting the respective MBSs into their corresponding trendline equations, which were obtained from the overall calibration sensitivity graphs (Figure 11), base LOD values were calculated. As previously explained, MBS values cannot be experimentally determined for real-time PCR; instead, MBSs unique to the application of the standard curve are employed. This means that two different MBS values will be used for real-time PCR: the mean male  $C_T$  value of the 0.023 ng (point “H”) calibration standard (36.00  $C_T$ ) and a  $C_T$  equal the highest value that the Quantifiler® Duo platform is set to detect (40  $C_T$ ). The experimentally determined MBSs for the RSID™ Saliva and RSID™ Semen cards are provided in Table 2; however, the following LOD analysis is not applicable for the RSID™ Semen cards due to the non-linearity of the calibration curve (Figure 11B).

Any meaningful approach to the determination of LODs must not only calculate the base LOD value but must also take into account its inherent error. In order to do this, Winefordner suggests utilizing the theory of Propagation of Random Error, which produces a more conservative estimate of the LOD than the graphical or IUPAC approaches by incorporating the error of the components, i.e. the calibration sensitivity, intercept of the calibration curve, and MBS [44]. To use this propagation of errors approach, a linear regression analysis of each of

the calibration curves was performed and the errors associated with the slopes and the intercepts obtained. For all MBSs, except the real-time PCR MBS of 40 C<sub>T</sub> that uses the previously described modeling approach, the errors were equivalent to one standard deviation of the mean.

Once the errors for each of the individual components were determined, they were used to propagate the error of the LODs. This was done in accordance with the theory of the propagation of random error [43, 45]:

$$\sigma_f^2 = \sum_{i=1}^K \left( \frac{\delta f}{\delta p_i} \sigma_{p_i} \right)^2 \quad (\text{Equation 6})$$

where  $p_i$  denotes a given parameter,  $\sigma_{p_i}$  is the error in  $p$ , and  $\sigma_f$  is the uncertainty produced by  $\sigma_{p_i}$ . By rearranging Equation 4, the general form of the trendline equations for each calibration curve is obtained:

$$c = e^{\frac{y-b}{m}} \quad (\text{Equation 7})$$

where  $y$  is the MBS,  $c$  is the concentration of the analyte,  $b$  is the intercept, and  $m$  is the slope. Note that Equation 7 takes into account the logarithmic relationship between the signal output and volume of body fluid. By substituting Equation 7 into Equation 6, partially differentiating with respect to each parameter ( $y$ ,  $m$ , and  $b$ ), and assuming the errors are independent, the following derivation is obtained:

$$\sigma_c^2 = \left( \frac{\delta c}{\delta y} \sigma_y \right)^2 + \left( \frac{\delta c}{\delta b} \sigma_b \right)^2 + \left( \frac{\delta c}{\delta m} \sigma_m \right)^2$$

then

$$\sigma_c^2 = \left( e^{\frac{y-b}{m}} \cdot \frac{1}{m} \cdot \sigma_y \right)^2 + \left( e^{\frac{y-b}{m}} \cdot \left( -\frac{1}{m} \right) \cdot \sigma_b \right)^2 + \left( e^{\frac{y-b}{m}} \cdot \frac{b-y}{m^2} \cdot \sigma_m \right)^2$$

then

$$\sigma_c^2 = \frac{e^{2\left(\frac{y-b}{m}\right)}}{m^2} \cdot \sigma_y^2 + \frac{e^{2\left(\frac{y-b}{m}\right)}}{m^2} \cdot \sigma_b^2 + e^{2\left(\frac{y-b}{m}\right)} \cdot \frac{(b-y)^2}{m^4} \cdot \sigma_m^2$$

then

$$\sigma_c^2 = \frac{e^{2\left(\frac{y-b}{m}\right)}}{m^2} \left( \sigma_y^2 + \sigma_b^2 + \left( \frac{b-y}{m} \right)^2 \sigma_m^2 \right)$$

then

$$\sigma_c = \frac{e^{\frac{y-b}{m}}}{m} \sqrt{\sigma_y^2 + \sigma_b^2 + \left( \frac{b-y}{m} \right)^2 \sigma_m^2} \quad (\text{Equation 8})$$

Note, the  $y$  term in Equation 8 is in units of  $C_T$  for Quantifiler® Duo and gray scale intensity for the immunoassay cards. By substituting the parameters and their associated errors into Equation 8, the standard deviation of each of the LODs was calculated. Three times the standard deviation, with respect to the LOD, was added to the base LOD value, which was previously determined through substitution of the appropriate MBS values into their corresponding calibration curves, to arrive at the overall LODs displayed in Table 11.

**Table 11.** Limits of Detection of saliva and semen for the various detection methods.

Sample Type	LOD <sub>cards</sub>	LOD <sub>Duo H</sub>	LOD <sub>Duo 40</sub>	Microscopic Sperm Search
Saliva	0.05 µL	0.31 µL	0.03 µL	N/A
Semen	---	0.02 µL	0.001 µL	0.3 µL

As seen in Table 11, no LOD could be calculated for the RSID™ Semen cards due to the high-dose hook effect, which caused the calibration curve to have a non-linear trendline. However, LODs for semen using the Quantifiler® Duo platform could be calculated and were several times lower than any of the LODs for saliva, which was expected and implies a higher concentration of the biological components in semen. Not surprisingly, the LODs for Quantifiler® Duo where the MBS equal to 40 C<sub>T</sub> was used were much lower than the LODs based off of the 0.023 ng (point “H”) calibration standard. The LOD for saliva on the RSID™ immunochromatographic test strips was comparable to that of Quantifiler® Duo, though Quantifiler® Duo with the 40 C<sub>T</sub> MBS was slightly less. Note, the LOD listed for the microscopic sperm search is taken from the lowest dilution on the +/- chart (Table 10) where all slides gave a positive reading.

These findings are corroborated by the RSID™ Saliva manufacturer’s LOD of less than 1 µL of human saliva, while another independent study found the LOD of the RSID™ Saliva cards to be 10 nL of human saliva [32, 46]. The result in Table 11 for the RSID™ Saliva cards (0.05 µL human saliva) falls between both of these reported values. Due to the lack of a numerical result, the same comparison cannot be made for the RSID™ Semen cards. LODs for the RSID™ Semen cards are reported, however, by other authors, including the somewhat contradictory values of 2.5 nL of human semen from the RSID™ developmental validation and 1 µL of human semen from information obtained from the manufacturer recommended protocol [15, 33].

An additional study reports that human semen and human seminal fluid standard could both be detected by the RSID™ Semen cards up to a 100,000 fold dilution [47], and yet another study that employed a different lateral flow immunochromatographic test strip to detect semenogelin in human semen had a similar outcome, with a reported LOD up to a dilution of 200,000 fold [48]. Unfortunately, in neither of these two studies did the authors describe the initial volume of semen or human seminal fluid standard used to make their dilution series, which makes interlaboratory comparisons difficult. Interlaboratory comparison using the Quantifiler® Duo LODs generated from this study would also be somewhat complicated, but not impossible, due to the fact that the forensic biology community most often reports their LOD findings in terms of concentration of DNA. The focus in this study was to choose a method that would allow for comparison between the RSID™ immunoassay cards and real-time PCR, therefore, LODs had to be calculated in terms of volume of body fluid of interest. If Figure 11 plotted  $C_T$  verse the log of the concentration of DNA, instead of the log of the volume of body fluid, LODs could be converted from units of volume into units of concentration, which would be comparable to the literature. For example, the Quantifiler® Duo developmental validation concludes that reproducible results can be obtained down to 11.5 pg/μL of DNA [49], a finding which is consistent with other publications that cite the LOD for analogous real-time PCR chemistries in the range of 100 fg to 0.1 ng of DNA [50-56]. However, the quoted LODs were not derived using MBS values and the

propagation of random errors, as was done in this study. The general approach seems to have been to create a DNA dilution series and analyze several replicates of that series using real-time PCR. It appears that in most cases, the LODs were then reported as the lowest concentration in the dilution series that yielded reproducible, positive results.

Numerous non-forensic applications of both lateral flow immunochromatographic test strips and real-time PCR have also been reported, and these publications support that both methods are highly selective with low LODs. For instance, immunoassay cards have been used in the fields of environmental and health sciences to detect analytes from fumonisins, a class of mycotoxins in maize, with an LOD of 120  $\mu\text{g/L}$  [34] to cortisol, a stress hormone in serum, with an LOD of 30 ng/mL [35]. Interestingly, in a paper by Tian et al. [31], the immunoassay card LOD of nortestosterone obtained after analysis with ImageJ (5 ng/mL) was 40 fold less than the LOD obtained by visual inspection (200ng/mL), as was the case in this study where the LOD calculated using propagation of random error and the MBS resulted in a LOD of 0.05  $\mu\text{L}$  (Table 11), while the LOD from visual inspection was 0.12  $\mu\text{L}$  (Table 9). As for real-time PCR, bacterial and viral studies aimed at detection and quantification have benefitted from the associated low LODs. For example, one study of *Salmonella* in biological specimens found the LOD of their real-time PCR system to be 250 copies/mL [57], and a second study of HPV in genital and oral samples found the LOD of their real-time PCR system to be 2 copies/reaction [58]. Although not

reported in the same manner, the totality of these literature findings are consistent with and support the overall low LOD results obtained from the RSID™ immunoassay cards and Quantifiler® Duo.

### *Reproducibility*

One last factor was considered in the evaluation of the RSID™ lateral flow immunochromatographic test strips and real-time PCR using the Quantifiler® Duo platform, and that was the reproducibility of the systems. In order to make this assessment, one-sided F-tests, which are statistical comparisons between the random errors of two data sets, were performed [43]. An F-test considers the ratios of the variances of two sample populations [43]:

$$F_{test} = \frac{s_1^2}{s_2^2} \quad (\text{Equation 9})$$

Using Equation 9,  $F_{test}$  values are calculated and compared to a critical value of  $F$ , usually obtained from a table of  $F_{crit}$  values that takes into account the level of significance of the test ( $P$ ) and the degrees of freedom of the sample populations. If the value of  $F_{test}$  is greater than the value for  $F_{crit}$ , the null hypothesis is rejected. In this case, the null hypothesis is  $H_0: \sigma_1^2 = \sigma_2^2$ , meaning that the variances of the two sample populations are not significantly different [43]. F-tests are typically conducted at a 5% level of significance ( $P = 0.05$ ), which indicates that there is a 5% chance of committing a type I error, or that the null hypothesis will be rejected when it is in fact true [43]. See Table 12 below for a complete listing of  $F_{test}$  values that compare the RSID™ immunoassay card variances with the corresponding Quantifiler® Duo variances.



**Table 12.**  $F_{test}$  values comparing sample variance seen on RSID™ immunoassay cards with the corresponding Quantifiler® Duo sample variance.

$F_{crit} = 3.204$		
Dilution	$F_{test}$ Saliva	$F_{test}$ Semen
Neat	117.4	7.148
1:2	383.5	148.3
1:5	1050	104.3
1:10	900.1	211.6
1:20	1414	25.04
1:50	2569	15.03
1:100	3776	398.4
1:250	134.8	96.99
1:500	43.28	999.3
1:750	50.52	407.4
1:1000	39.21	179.1

From the data in Table 12, the null hypothesis should be rejected for all of the F-tests. This suggests the variance associated with the RSID™ immunoassay cards is not equal to the variance in Quantifiler® Duo, and since Quantifiler® Duo variances were the smaller of the two, it is a more precise quantification method than RSID™ immunoassay cards analyzed with ImageJ. For the saliva dilutions series, however, the  $F_{test}$  values were much closer to  $F_{crit}$  toward the 1:1000 end of the dilution series, which is again evidence of the presence of stochastic effects during amplification. Stochastic effects were less noticeable for the semen series, which indicates a higher concentration of the biological components in semen than saliva, even when highly diluted.

The above F-tests only take into account the absolute standard deviations for the two methods. Since the units of signal and the signal magnitudes differ between the immunoassay cards and real-time PCR, as seen by the scales in

Figure 11, a meaningful comparison of their errors should also include their Relative Standard Deviations (RSD), which ensures that more emphasis is not placed on the error of one method over the other. The formula for RSD is [43]:

$$RSD = \frac{s}{\bar{x}} 100\% \quad (\text{Equation 10})$$

where the RSD has units of percent. In Equation 10,  $s$  is the sample standard deviation and  $\bar{x}$  is the sample mean. Figure 12, which plots RSID™ immunoassay card relative standard deviations against Quantifiler® Duo relative standard deviations, confirms the F-test findings seen in Table 12. From Figure 12, it is clear that the immunoassay cards have higher RSDs than real-time PCR, in every case except the neat semen samples, suggesting that Quantifiler® Duo is a more precise quantification method than RSID™ immunoassay cards analyzed with ImageJ.

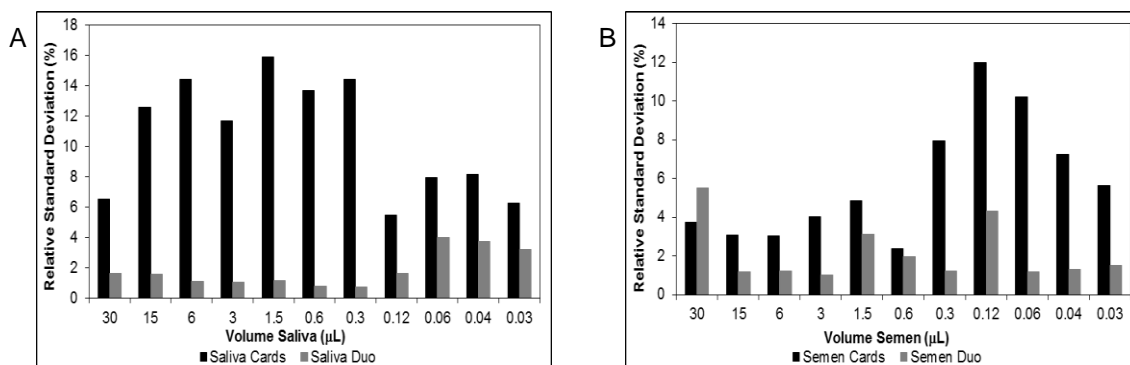


**Figure 12.** RSID™ immunoassay card RSDs plotted against Quantifiler® Duo RSDs. (A) Overall Saliva and (B) Overall Semen.

## Conclusions & Future Work

The question with the broadest implications to be answered by this research is whether or not forensic laboratories can replace body fluid identification tests, like the RSID™ lateral flow immunochromatographic test strips for saliva and semen, with a real-time PCR platform, like Quantifiler® Duo. In order to answer this question, several variables were examined and compared between the two methods including stability in different matrices, sensitivity, limit of detection, and reproducibility. It was found that determining the presence of saliva and the presence of semen were unaffected by sample matrix, i.e. blood and TE, for both methods; however, the ability to detect semen at high concentrations with the immunoassay cards was significantly diminished by the high-dose hook effect. Although Quantifiler® Duo cannot give information with respect to body fluid type, it consistently gave lower LODs than the immunoassay cards, was not affected by matrix, was able to detect DNA from samples with low sperm counts, and showed less variability between measurements. Due to its stability in various matrices, sensitivity, low LODs, and increased precision over the immunoassay cards, Quantifiler® Duo is a viable and effective screening method for subsequent DNA profiling.

Because Quantifiler® Duo cannot distinguish between body fluids, per se, its greatest impact would be felt in an analytical scheme where gender differences could be exploited such as with sexual assault cases, where the overwhelming majority of victims are female and the perpetrators are male [2].

One could imagine two different ways, dictated by the rule of law, to incorporate Quantifiler® Duo screening into current workflow practices. If the charge is not determined by the identification of a specific body fluid, then all sexual assault samples could be differentially extracted followed by quantification with Quantifiler® Duo. Only samples positive for male DNA would proceed to amplification. However, if the presence of different body fluids, i.e. semen verses saliva, alters the chargeable offense, a portion of the evidence could be saved for later testing with immunoassay cards. Returning to the remaining evidence for body fluid identification should not overburden the system because fewer samples would need to be screened than are currently. This would primarily be attributed to two factors: 1) a number of cases would certainly be halted due to a lack of male genetic material, and 2) many cases do not have previously identified suspects. In the later scenario, finding male DNA in a female body cavity may still indicate a that a crime has occurred. Any resulting genetic profile could be uploaded to CODIS without prior body fluid identification, and if a suspect was connected in the future, the body fluid identification could be made on the remaining evidence prior to trial.

Some forensic laboratories may be unwelcoming of the proposed analysis scheme because, without prior biological screening, it would increase the number of samples to be differentially extracted and quantified by the DNA unit. To combat this concern, one area of future research could work to increase throughput by automating differential extractions. Also, there is promising

research in the literature regarding the incorporation of mRNA profiling into a multiplex real-time PCR assay. This would have the potential to make current methods of body fluid identification obsolete [59-67]. With such advances on the horizon, replacing biological fluid identification via lateral flow immunochromatographic test strips with a real-time PCR chemistry for all biological cases is possible.

## Bibliography

### List of Abbreviated Journal Titles (In Alpha Order)

Anal. Biochem.	Analytical Biochemistry
Anal. Bioanal. Chem.	Analytical & Bioanalytical Chemistry
Anal. Chem.	Analytical Chemistry
Anal. Chim. Acta	Analytica Chimica Acta
Biol. Reprod.	Biology of Reproduction
Biotechnol.	Bio/Technology
BMC Biotechnol.	BioMed Central Biotechnology
BMC Infect. Dis.	BioMed Central Infectious Disease
Food Agr. Immunol.	Food and Agricultural Immunology
Forens. Sci.	Forensic Science
Forensic Sci. Int.	Forensic Science International
Int. J. Legal Med.	International Journal of Legal Medicine
J. Androl.	Journal of Andrology
J. Forensic Sci.	Journal of Forensic Science
J. Forensic Sci. Soc.	Journal of the Forensic Science Society
J. Immunol. Methods	Journal of Immunological Methods
Nature Biotechnol.	Nature Biotechnology
Nucleic Acids Res.	Nucleic Acids Research

Proc. Natl. Acad. Sci. USA

Proceedings of the National

Academy of Sciences of the

United States of America

Pure & Appl. Chem.

Pure and Applied Chemistry

Viol. J.

Virology Journal

- [1] Federal Bureau of Investigation, Quality Assurance Standards for Forensic DNA Testing Laboratories, Effective July 1, 2009, <http://www.fbi.gov/hq/lab/html/codis1.htm> .
- [2] U.S. Department of Justice – Federal Bureau of Investigation, Uniform Crime Report, Crime in the United States, 2009, <http://www2.fbi.gov/ucr/cius2009/index.html>.
- [3] Massachusetts State Police, Forensic Services Group, Forensic Biology – Criminalistics Unit, Examination of Sexual Assault Evidence Collection Kits, CRIM-01, version 5.1, Effective Date: April 10, 2007.
- [4] Massachusetts State Police, Forensic Services Group, Forensic Biology – Criminalistics Unit, Extraction of Sperm Cells and Body Fluids from Substrates, CRIM-02A, version 2.2, Effective Date: July 21, 2006.
- [5] Massachusetts State Police, Forensic Services Group, Forensic Biology – Criminalistics Unit, Microscopic Examination of Sperm Cells Using Hematoxylin and Eosin or Kernechtrot-Picroindigocarmine (Christmas Tree) Stains, CRIM-03, version 2.1, Effective Date: March 1, 2006.
- [6] Massachusetts State Police, Forensic Services Group, Forensic Biology – Criminalistics Unit, Procedure for the Determination of Human Salivary  $\alpha$ -Amylase, CRIM-24, version 2.0, Effective Date: April 6, 2009.
- [7] Massachusetts State Police, Forensic Services Group, Forensic Biology – Criminalistics Unit, Identification of Seminal Fluid Using the Rapid Stain Identification (RSID™) Test for Semen, CRIM-25, version 1.0, Effective Date: January 1, 2007.
- [8] G.M. Willott, Frequency of Azoospermia, Forensic Sci. Int. 20 (1982) 9-10.
- [9] National Institute of Health, The ImageJ User Guide, version 1.43, April 2010, <http://rsbweb.nih.gov/ij/>.

- [10] H.R. Horton, L.A. Moran, R.S. Ochs, J.D. Rawn, K.G. Scrimgeour, Principles of Biochemistry, third ed., Prentice Hall, Upper Saddle River, New Jersey, 2002.
- [11] R. Li, Forensic Biology, CRC Press, Taylor & Francis Group, Boca Raton, Florida, 2008.
- [12] W. Zhao, M.M. Ali, S.D. Aguirre, M.A. Brook, Y. Li, Paper-Based Bioassays Using Gold Nanoparticle Colorimetric Probes, Anal. Chem. 80 (2008) 8431-8437.
- [13] C. Sonnichsen, B.M. Reinhard, J. Liphardt, A.P. Alivisatos, A Molecular Ruler Based on Plasmon Coupling of Single Gold and Silver Nanoparticles, Nature Biotechnol. 23 (6) (2005) 741-745.
- [14] R. Tanaka, T. Yuhi, N. Nagatani, T. Endo, K. Kerman, Y. Takamura, E. Tamiya, A Novel Enhancement Assay for Immunochromatographic Test Strips Using Gold Nanoparticles, Anal. Bioanal. Chem. 385 (2006) 1414-1420.
- [15] Independent Forensics, Rapid Stain Identification of Human Semen (RSID™ – Semen), Technical Information and Protocol Sheet for Use with Dual Buffer System, Cat# 0200, February 2010, <http://www.ifit-test.com/rsid.php>.
- [16] R.K. Saiki, D.H. Gelfand, S. Stoffel, S.J. Scharf, R. Higuchi, G.T. Horn, K.B. Mullis, H.A. Erlich, Primer-Directed Enzymatic Amplification of DNA with a Thermostable DNA Polymerase, Science 239 (1988) 487-491.
- [17] J.M. Butler, Forensic DNA Typing, second ed., Elsevier Academic Press, Boston, 2005.
- [18] J.A. Sanchez, J.D. Abramowitz, J.J. Salk, A.H. Reis Jr., J.E. Rice, K.E. Pierce, L.J. Wangh, Two-Temperature LATE-PCR Endpoint Genotyping, BMC Biotechnol. 6 (44) (2006) 14 pages.
- [19] R. Higuchi, C. Fockler, G. Dollinger, R. Watson, Kinetic PCR Analysis: Real-Time Monitoring of DNA Amplification Reactions, Biotechnol. 11 (1993) 1026-1030.
- [20] P.M. Holland, R.D. Abramson, R. Watson, D.H. Gelfand, Detection of Specific Polymerase Chain Reaction Product by Utilizing the 5' → 3' Exonuclease Activity of *Thermus aquaticus* DNA Polymerase, Proc. Natl. Acad. Sci. USA 88 (1991) 7276-7280.



- [21] I.V. Kutyavin, I.A. Afonina, A. Mills, V.V. Gorn, E.A. Lukhtanov, E.S. Belousov, M.J. Singer, D.K. Walburger, S.G. Lokhov, A.A. Gail, R. Dempcy, M.W. Reed, R.B. Meyer, J. Hedgpeth, 3'-Minor Groove Binder-DNA Probes Increase Sequence Specificity at PCR Extension Temperatures, *Nucleic Acids Res.* 28 (2) (2000) 655-661.
- [22] Applied Biosystems, Quantifiler® Duo DNA Quantification Kit User's Manual, PN4391294, Rev. B, April 2008.
- [23] Independent Forensics, Rapid Stain Identification of Human Saliva (RSID™ – Saliva), Technical Information and Protocol Sheet for Use with Dual Buffer System, Cat# 0100, February 2010, <http://www.ifit-test.com/rsid.php>.
- [24] I. Koukoulas, F.E. O'Toole, P. Stringer, R.A.H. van Oorschot, Quantifiler™ Observations of Relevance to Forensic Casework, *J. Forensic Sci.* 53 (1) (2008) 135-141.
- [25] M.J. Auvdel, Amylase Levels in Semen and Saliva Stains, *J. Forensic Sci.* 31 (2) (1986) 426-431.
- [26] H. Koistinen, T. Soini, J. Leinonen, C. Hyden-Granskog, J. Salo, M. Halttunen, U.H. Stenman, M. Seppala, R. Koistinen, Monoclonal Antibodies, Immunofluorometric Assay, and Detection of Human Semenogelin in Male Reproductive Tract: No Association with In Vitro Fertilizing Capacity of Sperm, *Biol. Reprod.* 66 (2002) 624-628.
- [27] K. Yoshida, T. Yamasaki, M. Yoshiike, S. Takano, I. Sato, T. Iwamoto, Quantification of Seminal Plasmid Motility Inhibitor/Semenogelin in Human Seminal Plasma, *J. Androl.* 24 (6) (2003) 878-884.
- [28] S.M. Keating and D.F. Higgs, The Detection of Amylase on Swabs from Sexual Assault Cases, *J. Forensic Sci. Soc.* 34 (2) (1994) 89-93.
- [29] J. Kenna, M. Smyth, L. McKenna, C. Dockery, S.D. McDermott, The Recovery and Persistence of Salivary DNA on Human Skin, *J. Forensic Sci.* 56 (1) (2011) 170-175
- [30] A. Davies and E. Wilson, The Persistence of Seminal Constituents in the Human Vagina, *Forens. Sci.* 3 (1974) 45-55.

- [31] Z. Tian, L.Q. Liu, C. Peng, Z. Chen, C. Xu, A New Development of Measurement of 19-Nortestosterone by Combining Immunochromatographic Strip Assay and ImageJ Software, *Food Agr. Immunol.* 20 (1) (2009) 1-10.
- [32] J.B. Old, B.A. Schweers, P.W. Boonlayangoor, K. A. Reich, Developmental Validation of RSID™-Saliva: A Lateral Flow Immunochromatographic Strip Test for the Forensic Detection of Saliva, *J. Forensic Sci.* 54 (4) (2009) 866-873.
- [33] J. Old, B. Schweers, P.W. Boonlayangoor, K. Reich, Developmental Validation Studies of RSID™-Semen A Lateral Flow Immunochromatographic Strip Test for the Forensic Detection of Seminal Fluid, *Rev. D3, Independent Forensics*, 2010, <http://www.ifi-test.com/rsid.php>.
- [34] L. Anfossi, M. Calderara, C. Baggiani, C. Giovannoli, E. Arletti, G. Giraudi, Development and Application of a Quantitative Lateral Flow Immunoassay for Fumonisin in Maize, *Anal. Chim. Acta* 682 (2010) 104-109.
- [35] S. Nara, V. Tripathi, H. Singh, T.G. Shrivastav, Colloidal Gold Probe Based Rapid Immunochromatographic Strip Assay for Cortisol, *Anal. Chim. Acta* 682 (2010) 66-71.
- [36] D.A. Skoog, F.J. Holler, T.A. Neman, *Principles of Instrumental Analysis*, fifth ed., Harcourt Brace College Publishers, Philadelphia, 1998.
- [37] H. Kaiser, Quantitation in Elemental Analysis, *Anal. Chem.* 42 (2) (1970) 24A-41A.
- [38] H. Kaiser, Part II Quantitation in Elemental Analysis, *Anal. Chem.* 42 (4) (1970) 26A-59A.
- [39] Massachusetts State Police, Forensic Services Group, Forensic Biology – DNA Unit, Alternative Standard Dilution Series for DNA Quantification, Internal Validation, Approved: March 2007, 7 pages.
- [40] Massachusetts State Police, Forensic Services Group, Forensic Biology – DNA Unit, Validation of Applied Biosystems 7500 Real-Time PCR System: Summaries, Internal Validation, Approved: March 2007, 39 pages.

- [41] International Union of Pure and Applied Chemistry (IUPAC) – Analytical Chemistry Division Commission on Analytical Nomenclature, Nomenclature in Evaluation of Analytical Methods Including Detection and Quantification Capabilities, *Pure & Appl. Chem.* 67 (10) (1995) 1699-1723.
- [42] Scientific Working Group on DNA Analysis Methods (SWGDAM), SWGDAM Interpretation Guidelines for Autosomal STR Typing by Forensic DNA Testing Laboratories, 2010, <http://www.fbi.gov/about-us/lab/codis/swgdam-interpretation-guidelines>.
- [43] J.N. Miller and J.C. Miller, *Statistics and Chemometrics for Analytical Chemistry*, fourth ed., Prentice Hall, New York, 2000.
- [44] G.L. Long and J.D. Winefordner, Limit of Detection A Closer Look at the IUPAC Definition, *Anal. Chem.* 55 (7) (1983) 712-724.
- [45] C.M. Grgicak, Z.M. Urban, R.W. Cotton, Investigation of Reproducibility and Error Associated with qPCR Methods using Quantifiler<sup>®</sup> Duo DNA Quantification Kit, *J. Forensic Sci.* 55 (5) (2010) 1331-1339.
- [46] B.C.M. Pang and B.K.K. Cheung, Applicability of Two Commercially Available Kits for Forensic Identification of Saliva Stains, *J. Forensic Sci.* 53 (5) (2008) 1117-1122.
- [47] B.C.M. Pang and B.K.K. Cheung, Identification of Human Semenogelin in Membrane Strip Test as an Alternative Method for the Detection of Semen, *Forensic Sci. Int.* 169 (2007) 27-31.
- [48] I. Sato, K. Kojima, T. Yamasaki, K. Yoshida, M. Yoshiike, S. Takano, T. Mukai, T. Iwamoto, Rapid Detection of Semenogelin by One-Step Immunochromatographic Assay for Semen Identification, *J. Immunol. Methods* 287 (2004) 137-145.
- [49] M. Barbisin, R. Fang, C.E. O'Shea, L.M. Calandro, M.R. Furtado, J.G. Shewale, Developmental Validation of the Quantifiler<sup>®</sup> Duo DNA Quantification Kit for Simultaneous Quantification of Total Human and Human Male DNA and Detection of PCR Inhibitors in Biological Samples, *J. Forensic Sci.* 54 (2) (2009) 305-319.
- [50] R.L. Green, I.C. Roinestad, C. Boland, L.K. Hennessy, Developmental Validation of the Quantifiler<sup>™</sup> Real-Time PCR Kits for the Quantification of Human Nuclear DNA Samples, *J. Forensic Sci.* 50 (4) (2005) 809-825.

- [51] J.A. Walker, D.J. Hedges, B.P. Perodeau, K.E. Landry, N. Stoilova, M.E. Laborde, J. Shewale, S.K. Sinha, M.A. Batzer, Multiplex Polymerase Chain Reaction for Simultaneous Quantitation of Human Nuclear, Mitochondrial, and Male Y-Chromosome DNA: Application in Human Identification, *Anal. Biochem.* 337 (2005) 89-97.
- [52] K.M. Horsman, J.A. Hickey, R.W. Cotton, J.P. Landers, L.O. Maddox, Development of a Human-Specific Real-Time PCR Assay for the Simultaneous Quantification of Total Genomic and Male DNA, *J. Forensic Sci.* 51 (4) (2006) 758-765.
- [53] J.A. Nicklas and E. Buel, Simultaneous Determination of Total Human and Male DNA Using a Duplex Real-Time PCR Assay, *J. Forensic Sci.* 51 (5) (2006) 1005-1015.
- [54] K.L. Swango, W.R. Hudlow, M.D. Timken, M.R. Buoncristiani, Developmental Validation of a Multiplex qPCR Assay for Assessing the Quantity and Quality of Nuclear DNA in Forensic Samples, *Forensic Sci. Int.* 170 (2007) 35-45.
- [55] J.G. Shewale, E. Schneida, J. Wilson, J.A. Walker, M.A. Batzer, S.K. Sinha, Human Genomic DNA Quantification System, H-Quant: Development and Validation for Use in Forensic Casework, *J. Forensic Sci.* 52 (2) (2007) 364-370.
- [56] M.D. Timken, K.L. Swango, C. Orrego, M.R. Buoncristiani, A Duplex Real-Time qPCR Assay for the Quantification of Human Nuclear and Mitochondrial DNA in Forensic Samples: Implications for Quantifying DNA in Degraded Samples, *J. Forensic Sci.* 50 (5) (2005) 1044-1060.
- [57] T.V.T Nga, A. Karkey, S. Dongol, H.N. Thuy, S. Dunstan, K. Holt, L.T.P. Tu, J.I. Campbell, T.T. Chau, N.V.V. Chau, A. Arjyal, S. Koirala, B. Basnyat, C. Dolecek, J. Farrar, S. Baker, The sensitivity of real-time PCR Amplification Targeting Invasive *Salmonella* serovars in Biological Specimens, *BMC Infect. Dis.* 10 (125) (2010) 9 pages.
- [58] W.T. Seaman, E. Andrews, M. Couch, E.M. Kojic, S. Cu-Uvin, J. Palefsky, A.M. Deal, J. Webster-Cyriaque, Detection and Quantification of HPV in Genital and Oral Tissues and Fluids by real-time PCR, *Viol. J.* 7 (194) (2010) 17 pages.
- [59] M. Bauer and D. Patzelt, A Method for Simultaneous RNA and DNA Isolation from Dried Blood and Semen Stains, *Forensic Sci. Int.* 136 (2003) 76-78.

- [60] M. Alvarez, J. Juusola, J. Ballantyne, An mRNA and DNA Co-Isolation Method for Forensic Casework Samples, *Anal. Biochem.* 335 (2004) 289-298.
- [61] M. Setzer, J. Juusola, J. Ballantyne, Recovery and Stability of RNA in Vaginal Swabs and Blood, Semen, and Saliva Stains, *J. Forensic Sci.* 53 (2) (2008) 296-305.
- [62] J. Juusola and J. Ballantyne, Messenger RNA Profiling: A Prototype Method to Supplant Conventional Methods for Body Fluid Identification, *Forensic Sci. Int.* 135 (2003) 85-96.
- [63] M. Bauer and D. Patzelt, Protamine mRNA as Molecular Marker for Spermatozoa in Semen Stains, *Int. J. Legal Med.* 117 (2003) 175-179.
- [64] J. Juusola and J. Ballantyne, Multiplex mRNA Profiling for the Identification of Body Fluids, *Forensic Sci. Int.* 152 (2005) 1-12.
- [65] C. Nussbaumer, E. Gharehbaghi-Schnell, I. Korschineck, Messenger RNA Profiling: A Novel Method for Body Fluid Identification by Real-Time PCR, *Forensic Sci. Int.* 157 (2006) 181-186.
- [66] M. Bauer and D. Patzelt, Identification of Menstrual Blood by Real Time RT-PCR: Technical Improvements and the Practical Value of Negative Test Results, *Forensic Sci. Int.* 174 (2008) 54-58.
- [67] A. Wasserstrom, D. Frumkin, A. Davidson, B. Budowle, Forensic Tissue Identification Based on DNA Methylation, *Proceedings of the American Academy of Forensic Sciences*, 17 (A59) (2011) 51-52.

## Curriculum Vitae

**Crystal Mae (Simson) Oechsle**

[cs207903@ohio.edu](mailto:cs207903@ohio.edu)

22 Waltham Street, Apt. A1  
Maynard, MA 01754

**Year of Birth:** 1985

**Education:** Ohio University, Athens, OH  
Bachelor of Science in Forensic Chemistry  
June 2007

Boston University, Boston, MA  
Master of Science in Biomedical Forensic Science  
May 2011

**Awards & Honors:** ΦBK National Honor Society  
OU Outstanding Forensic Chemist (2005 -2007)  
Provost's Undergraduate Research Grant Recipient  
American Chemical Society Analytical Award (2006)

**Published Work:** Means, J. A.; Wolf, Steffen; Agyeman, Akwasi;  
Burton, J. S.; Simson, C. M.; Hines, J. V. T Box  
Riboswitch Antiterminator Affinity Modulated by tRNA  
Structural Elements. *Chem. Biol. Drug Des.* **2007**, 69  
(2), 139-145.

**Presentations:** NEAFS 2010 Annual Meeting, Poster Session  
Crystal Simson Oechsle, Amy L. Barber, Sandra  
Haddad, Joanne B. Sgueglia, Catherine M. Grgicak.  
A Comparative Study of Biological Fluid Identification  
Methods: Lateral Flow Immunochromatographic Test  
Strips and Real-Time PCR Quantification using  
Quantifiler® Duo.

### Relevant Work Experience:

*June 2007 – present* Massachusetts State Police, Maynard, MA

*June – August 2006* NASA Glenn Research Center, Cleveland, OH